From the Rolf Luft Research Center for Diabetes and Endocrinology
Department of Molecular Medicine and Surgery
Karolinska Institutet, Stockholm, Sweden

PANCREATIC BETA-CELL INSULIN SIGNALING IN GENETIC AND DIETARY MODELS OF OBESITY AND INSULIN RESISTANCE

Meike Paschen

Stockholm 2019

Published by Karolinska Institutet.
Printed by E-Print AB 2019.

ISBN 978-91-7831-329-7

PANCREATIC BETA-CELL INSULIN SIGNALING IN GENETIC AND DIETARY MODELS OF OBESITY AND INSULIN RESISTANCE

THESIS FOR DOCTORAL DEGREE (Ph.D.)

By

Meike Paschen

Public defense on Friday the 22nd of March 2019 at 9:00 am
The Rolf Luft Auditorium, L1:00, Solna

Principal Supervisor:
Ingo B. Leibiger, Docent
Karolinska Institutet
Department of Molecular Medicine and Surgery

Co-supervisors:
Barbara Leibiger, Docent
Karolinska Institutet
Department of Molecular Medicine and Surgery

Per-Olof Berggren, Professor
Karolinska Institutet
Department of Molecular Medicine and Surgery

Opponent:
Peter Flatt, Professor
Ulster University
Biomedical Sciences Research Institute

Examination Board:
Anna Krook, Professor
Karolinska Institutet
Department of Physiology and Pharmacology

Ingrid Dahlman, Professor
Karolinska Institutet
Department of Medicine, Huddinge

Anders Tengholm, Professor
Uppsala University
Department of Medical Cell Biology

"Life is something you have to take care of- Don´t you realize that?"

Astrid Lindgren, Ronja, the Robber´s Daughter

To my family

ABSTRACT

Type 2 Diabetes Mellitus (T2DM) is a heterogeneous metabolic disease characterized by elevated blood glucose levels that has reached pandemic proportions. Genome-wide association studies have linked T2DM to the function of the insulin-producing pancreatic β-cell residing in the micro-organ islet of Langerhans. An individual´s risk to develop T2DM depends on genetic predisposition and environmental factors, e.g. life style. Central for disease development is the interplay between insulin resistance in insulin target tissues like muscle, liver and fat and deficient β-cell insulin secretion. Since the β-cell is an insulin target itself, β-cell insulin resistance can contribute to β-cell dysfunction and the development of T2DM. This was shown in several genetic (knockout) mouse models, however the dynamics of β-cell insulin resistance and its relevance in a diet-induced context has so far not been explored. Furthermore the consequences of diet-induced β-cell insulin resistance for β-cell function remain to be understood. The difficulty to study β-cell insulin resistance *in vivo* has partly been due to the lack of a technique to monitor β-cell insulin resistance non-invasively and longitudinally in the living organism.

In my thesis I employed the anterior chamber of the eye of mice as a transplantation site for biosensor-expressing reporter islets and the cornea as a natural body window to monitor β-cell insulin resistance non-invasively and longitudinally by microscopic imaging. The β-cell insulin resistance biosensor is based on GFP-labeled FoxO1, that changes its intracellular localization from cytoplasmic (insulin responsive) to nuclear (insulin resistant). With this technique we investigated β-cell insulin resistance dynamics in ob/ob and NZO mice and demonstrated that β-cell insulin resistance dynamics vary in animal models of insulin resistance and obesity. Furthermore, we showed that β-cell insulin resistance developed in the presence of whole-body insulin resistance, impaired glucose tolerance and increased body weight, but independently from liver insulin resistance. To study the relevance of β-cell insulin resistance in diet-induced T2DM development, we treated diabetes-prone male C57BL/6J mice with different combinations of solid high fat diet and drinking water containing either sucrose or fructose. Employing our new monitoring technique we showed that only mice that were fed a High-Fat-High-Sucrose-Diet developed β-cell insulin resistance. This demonstrated the importance of β-cell insulin resistance in a model of diet-induced obesity and insulin resistance and highlighted the importance of diet composition for the development of T2DM. The β-cell insulin resistance was accompanied by a decreased functional β-cell mass and impaired insulin secretion downstream of glucose-stimulated Ca^{2+} influx, due to a reduction of syntaxin-1A. We were also able to show that β-cell insulin resistance in one insulin signaling cascade can re-route the insulin signal, thus allowing the co-existence of reduced and increased insulin response in the same cell.

In conclusion, my *in vivo* studies of diet-induced β-cell insulin resistance and its consequences on β-cell function and survival contribute to better understanding of the development of T2DM.

PUBLICATIONS INCLUDED IN THIS THESIS

I. Meike Paschen, Tilo Moede, Barbara Leibiger, Stefan Jacob, Galyna Bryzgalova, Ingo B. Leibiger, and Per-Olof Berggren. **Non-invasive cell type selective in vivo monitoring of insulin resistance dynamics.** Scientific Reports. 6, 21448; doi: 10.1038/srep21448 (2016).

II. Meike Paschen*, Tilo Moede*, Ismael Valladolid-Acebes, Barbara Leibiger, Noah Moruzzi, Stefan Jacob, Concha F. García-Prieto, Kerstin Brismar, Ingo B. Leibiger, and Per-Olof Berggren. **Diet-induced β-cell insulin resistance results in reversible loss of functional β-cell mass.** FASEB J. 33, 204-218; doi: 10.1096/fj.201800826R. (2019)

*contributed equally

III. Barbara Leibiger, Tilo Moede, Meike Paschen, Na-Oh Yunn, Jong Hoon Lim, Sung Ho Ryu, Teresa Pereira, Per-Olof Berggren, and Ingo B. Leibiger. **PI3K-C2α Knockdown Results in Rerouting of Insulin Signaling and Pancreatic Beta Cell Proliferation.** Cell Reports 13, 15–22; doi: 10.1016/j.celrep.2015.08.058. (2015).

Some additional data that have not been published previously are included in the results and discussion chapter (chapter 5).

PUBLICATIONS NOT INCLUDED IN THIS THESIS

I. Karin Åvall, Yusuf Ali, Ingo B. Leibiger, Barbara Leibiger, Tilo Moede, Meike Paschen, Andrea Dicker, Elisabetta Daré, Martin Köhler, Erwin Ilegems, Midhat H. Abdulreda, Mark Graham, Rosanne M. Crooke, Vanessa S. Y. Tay, Essam Refai, Stefan K. Nilsson, Stefan Jacob, Lars Selander, Per-Olof Berggren, and Lisa Juntti-Berggren. **Apolipoprotein CIII links islet insulin resistance to β-cell failure in diabetes.** Proc. Natl. Acad. Sci. USA 112, E2611–E2619; doi: 10.1073/pnas.1423849112. (2015).

Content

ABBREVIATION LIST

ACE- Anterior chamber of the eye

ADP- Adenosine di-phosphate

Akt- Protein kinase B

ATP- Adenosine tri-phosphate

AUC- Area under the curve

B6 mice- C57BL/6J mice

βFLUOMETRI- β-cell fluorescent metabolic transcriptional response indicator

BG- Background

βIRB- β-cell insulin resistance biosensor

βIRKO mouse- β-cell insulin receptor specific knockout mouse

BrdU- Bromodeoxyuridine

BSA- Bovine serum albumin

CFP- Cyan fluorescent protein

CMV- Cytomegalovirus

DAPI- 4',6-diamidino-2-phenylindole

DMEM- Dulbecco′s modification of Eagle′s medium

dsRed- Discosoma sp. Red fluorescent protein

EDTA- Ethylene diamine tetra-acetic acid

EGTA- Ethylene glycol-bis(2-aminoethylether)-N,N,N′,N′-tetraacetic acid

EdU- 5-Ethynyl-2′-deoxyuridine

ERK1/2- Extracellular signal-regulated kinase 1/2

FBS- Fetal bovine serum

FRET- Fluorescence/Förster resonance energy transfer green

FoxO1- Forkhead box protein O1

$FoxO1_{cyt}$- Cytoplasmic FoxO1

$FoxO1_{nuc}$- Nuclear FoxO1

GCaMP- Ca^{2+}-indicator

GEFB- Genetically encoded fluorescent biosensor

GFP- Green fluorescent protein

GLUT1- Glucose transporter 1

GLUT2- Glucose transporter 2

Grb2- Growth factor receptor-bound protein 2

HbA1c- Glycated hemoglobin

HEK- Human embryonic kindney

HFD- High fat diet

HFrD- High fructose diet

HSD- High sucrose diet

HFHFrD- High fat high fructose diet

HFHSD- High fat high sucrose diet

IGF-I- Insulin like growth factor-I

i.p.- Intraperitoneal

IPGTT- Intraperitoneal glucose tolerance test

IPITT- Intraperitoneal insulin tolerance test

IPPTT- Intraperitoneal pyruvate tolerance test

IR-A- Insulin receptor A

IRES- Internal ribosome entry site

IR-B- Insulin receptor B

IRS-2- Insulin receptor substrate 2

JNK- c-Jun-N-terminal kinase

KO- Knockout

MEK1- MAP and ERK kinase 1

NZO mouse- New Zealand Obese mouse

p70s6k- Ribosomal p70 s6 kinase

PBS- Phosphate-buffered saline solution

Pdx1- Pancreatic and duodenal homeobox protein 1

PI3K Ia- Class IA Phosphatidylinositol 3-Kinase

PI3K-C2α- Phosphatidylinositol 3-kinase C2α

PMSF- Phenylmethane sulfonyl fluoride

rβIRI- Relative insulin resistance index

RIP- Rat insulin promoter

SDS- Sodium dodecyl sulfate

Shc- Src-homology 2 domain containing transforming protein 1

SNARE- Soluble N-ethylmaleimide attachment receptor

T1DM- Type 1 diabetes mellitus

T2DM- Type 2 diabetes mellitus

TBC1D4- TBC1 domain family member 4

3Tomato- Triple Tomato cDNA

TSC2- Tuberous Sclerosis Complex 2

YFP- Yellow fluorescent protein

1 INTRODUCTION

Type 2 Diabetes Mellitus (T2DM) is a heterogeneous disease that has reached pandemic proportions during the last decades, affecting around 9% of the adult population worldwide. It is characterized by elevated blood glucose levels due to relative insulin deficiency as the result of impaired insulin secretion and/or utilization. Consequences of chronically elevated blood glucose levels are manifold and include amongst others kidney failure, blindness as well as leg amputation and contribute to premature death. Both the genetic background and environmental factors have been identified as risk factors leading to huge variety of possible underlying mechanisms for disease development. Especially the increased intake of fast food, consisting of high amounts of sugar and fat, in combination with a sedentary life style, is believed to contribute to the rise in T2DM cases[1,2,3].

Genome-wide association studies have linked pancreatic β-cell function to T2DM[4]. The pancreatic β-cell within the micro-organ islet of Langerhans secretes insulin upon glucose stimulation. The interplay of insulin resistance in insulin target tissues, like muscle, liver and fat, with β-cell insulin secretion deficiency is seen as central for the disease development[5]. It has been shown that the β-cell is not only the site of insulin production, but also an insulin target tissue, where insulin signaling takes place[6]. Consequently also the β-cell can develop insulin resistance that potentially contributes to β-cell dysfunction and subsequently to the development of T2DM. Several genetic (knockout) mouse models have shown that a failure in β-cell insulin signaling due to the absence of a member of the insulin signaling cascade can lead to the development of β-cell insulin resistance[7–12]. The relevance of β-cell insulin resistance in a diet-induced context has so far not been investigated. One reason is the accessibility of β-cells in the pancreas for monitoring techniques. While it is possible to measure glucose and insulin tolerance non-invasively by tolerance tests, until now no method has been available to non-invasively monitor β-cell insulin sensitivity longitudinally *in vivo*.

A few years ago our group developed a technique to longitudinally and non-invasively monitor islets of Langerhans in mice[13,14]. There, pancreatic islets were transplanted to the anterior chamber of the eye (ACE) of mice, where they have been shown to become fully vascularized and innervated. Employing the cornea as a natural body window allowed to follow engrafted islets over time at cellular resolution by employing microscopic imaging. Since it has been shown that these islets report on the function of islets in the pancreas[15], the *in vivo* imaging platform gives the possibility to longitudinally study β-cells in islets of Langerhans *in vivo*. For investigation of specific functions and aspects, genetically encoded fluorescent biosensors can be used[16–18].

The aim of the present work was to develop and validate a method to study dynamics of β-cell insulin resistance *in vivo*, to explore the relevance of β-cell insulin resistance in the context of diet-induced T2DM development and furthermore to start to investigate the consequences of β-cell insulin resistance for β-cell function.

2 BACKGROUND

2.1 Diabetes mellitus

2.1.1 Definition, characteristics and epidemiology of diabetes mellitus

Diabetes mellitus is a heterogeneous metabolic disease that is characterized by increased blood glucose levels. In humans one of the following three different criteria is used for diagnosis: 1) fasting plasma glucose level of ≥ 7 mmol/l; 2) plasma glucose 2 hours after glucose stimulation is ≥ 11.1 mmol/l; 3) HbA1c ≥ 6.5%. The increased levels of blood glucose can be due to the failure or dysfunction of one or more processes involved in glucose homeostasis[1].

Already in 1906 a connection was seen between the proper function of pancreatic islets of Langerhans and the ability of the organism to maintain normal glucose concentration[19]. The islets of Langerhans were discovered by Paul Langerhans in 1869 and are situated in the pancreas there forming the endocrine part. It is a highly vascularized and innervated micro-organ consisting of different cell types: Non-endocrine dendritic, neuronal, Schwann and endothelial cells, pericytes, and macrophages as well as endocrine cells including the insulin producing β-cell, the glucagon producing α-cell, somatostatin releasing δ-cells as well as pancreatic polypeptide producing PP/γ-cells and ghrelin producing ε-cells. All endocrine islet cells release their hormones in response to multiple signals. The islet has a diameter of 50 to 280 µm and a healthy human has ca. 1 million islets, while a mouse has 3000-5000 islets. The hormone insulin is responsible for a lowering of blood glucose levels and produced by the β-cell[20]. Genome wide association studies have linked genes associated with diabetes to β-cell function[4]. In general insulin acts on various target tissues where it fulfills different functions all aiming to keep blood glucose levels in a physiological range[20]. Consequently a failure in one of these processes can lead to impaired glucose homeostasis and finally to diabetes.

Uncontrolled diabetes can lead to many different late complications such as neuropathy, nephropathy, micro- and macroangiopathy leading to amongst other things myocardial infarction, stroke, kidney failure, vision loss, leg amputation and it is one leading cause for premature death. 422 million adults were estimated to live with diabetes in 2014 and it was responsible for 1.5 million deaths in 2012 worldwide. Additionally 2.2 million deaths were reported to be related to higher-than-optimal blood-glucose levels. It is expected that these numbers will rise during the next decades[1,2].

2.1.2 Types of diabetes mellitus

Diabetes is currently divided into different subgroups and the categorization is based on the time and cause of onset. Type I Diabetes Mellitus (T1DM) is characterized by β-cell loss, resulting in absolute insulin deficiency and without any insulin treatment these patients cannot survive. The loss of β-cells is thought to be provoked by autoimmune disruption, but the exact cause for the disease is unknown and still under investigation. Regional differences in prevalence are seen, but also genetics and other environmental influences are risk factors for T1DM. Mostly children and adolescents are affected by T1DM[1,2]. Latent Autoimmune

Diabetes in Adults (LADA) is a form of diabetes that is caused by autoimmune disease, but it progresses slower than T1DM and is therefore often diagnosed in adults[21].

The present work focuses on T2DM. T2DM encompasses currently around 90% of diabetes cases worldwide. In contrast to T1DM, β-cells still remain and produce insulin in T2DM, but the amounts of secreted insulin are not sufficient to keep the blood glucose level within physiological range. This is most often due to insulin resistance of insulin target tissues, defined as the inability to use insulin effectively[22]. In response to insulin resistance of liver, muscle and fat, β-cells initially increase their insulin secretion. In humans a fasting plasma insulin concentration higher than 60 pmol/l[23] is considered as insulin resistance. As the disease progresses insulin secretion by the β-cells becomes defective and diabetes develops. Consequently, insulin resistance of the classical insulin target tissues in combination with impaired insulin secretion by the β-cell causes T2DM[5]. Since disease symptoms are less pronounced in T2DM, the disease can remain undiagnosed for years[1,2]. In general, underlying failures in insulin tolerance and secretion can be multifactorial and lead to differences in the disease characteristics of the individual level. New classifications to stratify patient groups with diabetes are currently under discussion[24].

Another type of diabetes mellitus is gestational diabetes only occurring during pregnancy when any degree of hyperglycemia is recognized for the first time[25].

2.1.3 Risk factors and prevention of Type 2 Diabetes Mellitus

Even if the underlying disease mechanisms cannot be addressed for each patient, risk factors for T2DM have been found and are used as a good starting point for diabetes prevention. The interplay between genetics and metabolic risk factors contributes to the individual risk to develop T2DM[26]. Family history of diabetes and ethnicity are risk factors that cannot be influenced, but it has been shown that a healthy life style can delay or prevent the onset of diabetes[27,28]. Healthy life style includes physical activity, avoidance of smoking and high consumption of alcohol. But highest emphasis is on the prevention of diabetes by adequate food and beverage consumption, avoiding high intake of saturated fatty acids and sugar, but encouraging the intake of fresh fruit, vegetables and fibres[1,2]. Here it has to be noted that the frequently used body mass index (BMI) cannot exclusively be used to measure someone's risk for the development of diabetes. One should consider additional measurements of several other parameters like the amount of visceral and subcutaneous fat, fitness and insulin sensitivity[29].

2.2 The pancreatic β-cell

The β-cell within the micro-organ islet of Langerhans is the site of insulin production, release and also of insulin signaling. Nerve stimulation, intra islet cell-cell communication, and humoral factors (hormones, vitamins, nutrients and more) play an important role in the regulation of β-cell function. Also paracrine signals from other pancreatic endocrine cell types influence the β-cell. Among others glucagon released from pancreatic α-cells stimulates insulin secretion and somatostatin secreted by pancreatic δ-cells suppresses insulin release. It has also been shown that the β-cell is an insulin target tissue. That was unexpected and controversially discussed, because the β-cell is thought to be permanently exposed to insulin. As an autocrine signal, insulin influences β-cell functions such as maintenance of β-cell mass, insulin biosynthesis and secretion in a short- and long-term dependent manner via insulin signaling through different pathways downstream of the insulin receptors. Variety of insulin signaling downstream of the insulin receptors is achieved by interaction of insulin receptors with different proteins involving different protein binding motifs within the receptor β-chains[6,30].

2.2.1 Insulin- "stimulus-secretion coupling"

Glucose is taken up by the β-cell via the insulin-independent Glucose transporter 2 (GLUT2) (mouse)/ Glucose transporter 1 (GLUT1) (human). Subsequent to phosphorylation by glucokinase, glucose is metabolized in glycolysis and further in the Krebs cycle. This results in a change in the Adenosine tri-phosphate (ATP)/ Adenosine di-phosphate (ADP) ratio in the cytoplasm and the closing of ATP/ADP-sensitive potassium channels. Since potassium ions no longer leave the cell, membrane depolarization occurs leading to opening of voltage-dependent L-type Ca^{2+}-channels. Ca^{2+} entering the cell promotes insulin exocytosis[31](Fig. 2.1).

2.2.2 Insulin signaling via insulin receptor-A and -B

Two different insulin receptor (IR) isoforms have been identified: Insulin receptor-A and -B (IR-A and IR-B). They differ in 12 amino acids in the C-terminus of the α-chain of the receptor, a result of alternative splicing of exon 11 of the IR transcript[32]. IR-A lacks exon 11[33] in contrast to IR-B that contains it[34]. Downstream of IR-A insulin regulates the expression of its own gene via a signaling cascade in a short-term manner. Insulin binding to the IR leads to its autophosphorylation by tyrosine kinase activity. The insulin receptor substrate 2 (IRS-2) recognizes the NPEY-motif of IR-A and mediates the receptor tyrosine kinase activity to Class IA Phosphatidylinositol 3-Kinase (PI3K Ia) and p70s6k as well as to Ca^{2+}/calmodulin-dependent protein kinase II (CaMKII) activities[35–37]. Downstream of IR-B two different pathways have been identified. Class IIA Phosphatidylinositol 3-Kinase (PI3K-C2α) recognizes the NPEY-motif of the receptor and mediates the signaling to Phosphoinositide-dependent kinase-1 (PDK1) and PKB/Akt which regulates glucokinase gene expression (Fig. 2.1). This signaling cascade is known as metabolic pathway of insulin signaling.

In the context of mitogenic effects on the other hand PI3K Ia binds to the YTHM-domain of the β-chain of the IR and is necessary for subsequent recruitment of p52-Shc to IR-B. Shc binds to the c-terminal YTHM-motif of the IR-B and the complex of IR-B/Shc is internalized into clathrin-coated vesicles. It has been shown that further Shc signaling derives from early endosomes, involving signaling via Grb2/Sos/Ras/Raf/MEK1/ERK1/2 leading to transcription of c-fos. This signaling cascade is known as mitogenic pathway of insulin signaling and triggers proliferation[37] (Fig. 2.1).

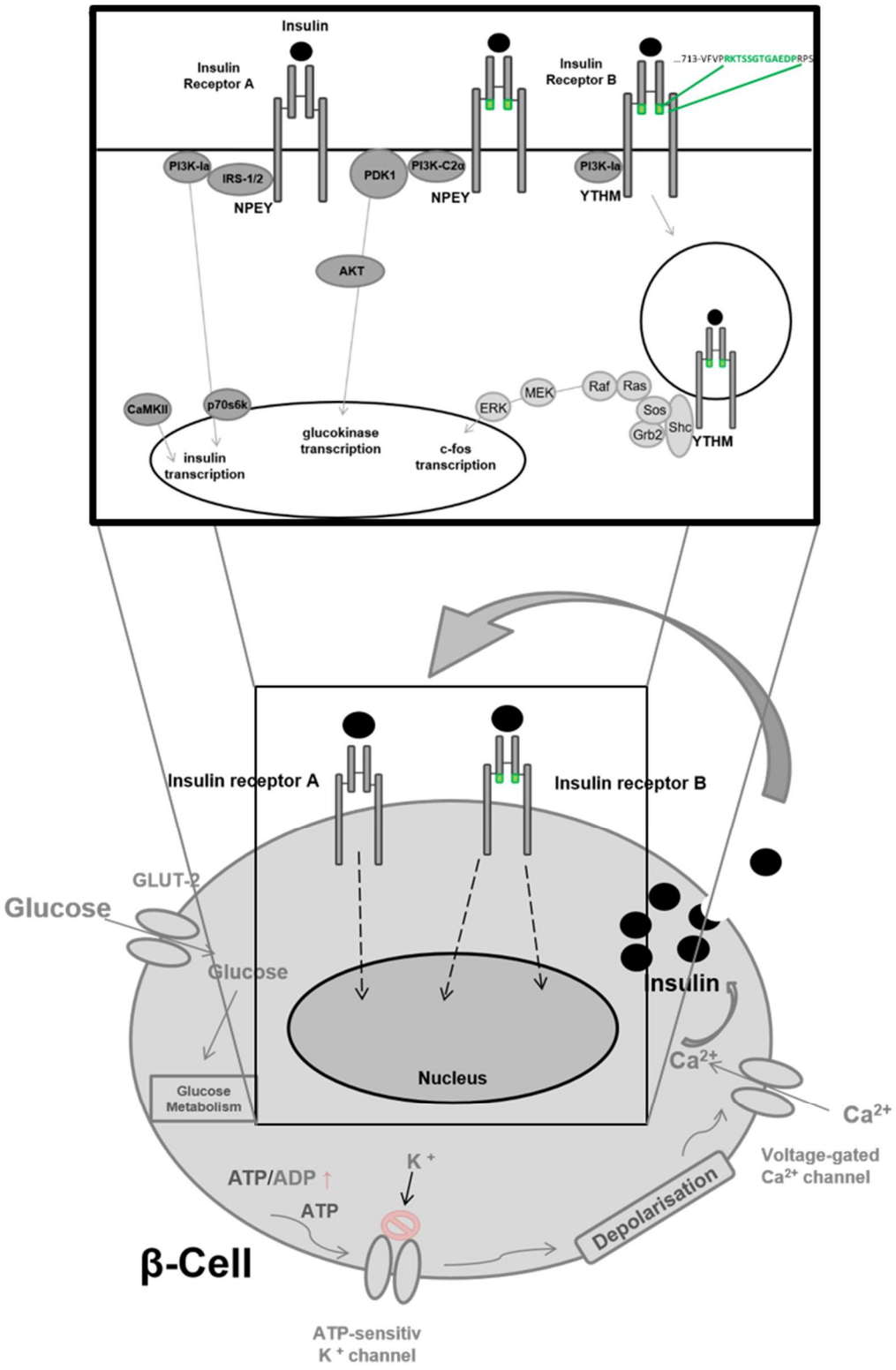

Figure 2.1.: The pancreatic β-cell

Increased glucose uptake and metabolism stimulates insulin secretion. Secreted insulin influences β-cell function through different pathways downstream of IR-A and -B in an autocrine manner.

2.2.3 β-cell insulin resistance

First evidence for the existence of β-cell insulin resistance and its relevance to glucose homeostasis, adequate insulin secretion and β-cell mass *in vivo*, came from β-cell-targeted manipulation of candidate genes playing a role in β-cell insulin signaling. A β-cell specific knockout (KO) of the IRs in βIRKO mice resulted in impaired glucose tolerance and reduced insulin secretion[7]. This mouse model demonstrated that a failure in β-cell insulin signaling, i.e. β-cell insulin resistance, can contribute to the development of T2DM. This was also shown in β-cell specific KO models of other members in the insulin signaling cascade, such as IRS-2[10], PI3K[12] and Akt[38], all displaying impairment of glucose-stimulated insulin secretion. Deeper analysis of the underlying molecular consequences of altered insulin signaling in KO mouse models gave further insights into the importance of β-cell insulin resistance/insulin sensitivity.

The lack of IRS-2 provoked a decrease in β-cell mass due to decreased proliferation and attenuated Ca^{2+} fluxes in response to glucose. Gene expression and protein analysis of β-cells from IRS-2 KO mice revealed a decrease in GLUT2, but maintained levels of the β-cell master regulator pancreatic and duodenal homeobox 1 (Pdx1) and of glucokinase[10]. This mouse model demonstrated the importance of IRS-2 and intact insulin signaling for maintenance of β-cell mass and regulation of insulin secretion. PI3K Ia deletion[12] affected downstream events of insulin signaling, resulting in nuclear localization and activation of the transcription factor forkhead box protein O1 (FoxO1). Here, both increased apoptosis and proliferation of β-cells were observed. A reduction in exocytotic events in combination with normal levels of cytosolic free Ca^{2+} ($[Ca^{2+}]_i$) suggested a defect downstream of the Ca^{2+} influx machinery. Gene expression analysis revealed maintained glucokinase levels, but a reduction in GLUT2 and Pdx1, going hand in hand with the nuclear localization of FoxO1. Furthermore a decrease in expression of soluble N-ethylmaleimide attachment receptor (SNARE) complex proteins was observed[12]. Reduced Akt activity in β-cells[38] led to impaired insulin secretion due to a defect in exocytosis independent from Ca^{2+} influx. β-cell mass was unaffected in these mice. The importance of the genetic background on the phenotypical outcome in mice was demonstrated when the same KO was introduced into mice with different genetic backgrounds resulting in great phenotypical variation[39]. Especially C57BL/6J (B6) mice were shown to be more prone to develop diabetes[40]. The observed effects in KO mice were similar in general (e.g. resulting in reduced glucose stimulated insulin secretion), but also different in detail, emphasizing the requirement to specify insulin resistance due to the complexity of the huge network of different insulin signaling pathways giving the possibility to cause insulin resistance in many different ways.

2.2.4 Forkhead box protein O1 (FoxO1)

FoxO1 is a transcription factor and the most abundant member of the family of Forkhead transcription factors regulating several different cell processes like proliferation, differentiation and survival in a broad spectrum of cell types[41,42]. It is evolutionary conserved and has important functions in the β-cell. FoxO1 phosphorylation and the resulting subcellular localization is regulated by glucose through IR signaling via the PI3K/Akt pathway[43] and by the c-Jun-N-terminal kinase (JNK) pathway[44]. Under normal, insulin responsive, conditions, FoxO1 is phosphorylated by Akt leading to its cytoplasmic localization. In case of failure in insulin signaling, i.e. insulin resistance, FoxO1 is no longer phosphorylated by Akt resulting in its translocation to the nucleus where it binds to its target genes promoting their expression[45]. Also oxidative stress can provoke FoxO1 nuclear localization by either acetylation by Cbp/p300-interacting trans-activator 1[46] or phosphorylation by JNK, at phosphorylation sites distinct from those of Akt[44].

Important FoxO1 target genes in the β-cell are the transcription factors MafA, NeuroD and Pdx1. MafA and NeuroD are important transcription factors in insulin expression, but also for β-cell differentiation during embryogenesis[46,47]. Pdx1 is one of the master transcription factors of the β-cell, regulating the expression of several β-cell genes, including GLUT2[48]. FoxO1 as a negative regulator of Pdx1 shows an opposite nuclear localization pattern[49].

2.3 The *in vivo* imaging platform

The ACE has been used as a transplantation site since the 19th century[50]. It is an immune privileged site allowing the proper survival of the transplant and the transparency of the cornea makes it a natural body window. Beside others, pancreatic tissue was transplanted to the ACE for morphological studies[51]. In 2008 the ACE was reported for the first time as a transplantation site for *in vivo* imaging of pancreatic islets of Langerhans[13,14]. For this, donor pancreatic islets are isolated, e.g. by collagenase digestion and subsequent handpicking (Fig. 2.2). Prior to transplantation the islets can be transduced with an adenovirus encoding a fluorescent biosensor (see 2.4). For transplantation, the recipient animal is anesthetized, a small hole is made into the cornea, and islets are gently injected and placed onto the iris. Normally syngeneic transplantations of age-matched islets are performed, but usage of immunocompromised mice allows also allogeneic or xenogeneic transplantation, the latter used for transplantation of human islets into mice[52]. After transplantation it takes approximately four weeks before the islets are fully vascularized[14] and 3 months to be fully innervated in the ACE[53,54]. The pancreatic islets can be monitored in the anesthetized recipient by different microscopic techniques depending on the scientific question. Laser scanning confocal microscopy for instance allows high-resolution at the (sub-) cellular level.

When the islets are vascularized the immune privilege of the anterior chamber is lost, and the islets are connected to the rest of the organism, allowing to draw conclusions from observations of islets in the ACE about conditions of the islets in the pancreas[15]. However, this has to be confirmed for every new biosensor.

In general, two main approaches are used for islet transplantation into the ACE. Firstly, metabolic transplantations where the islets in the eye replace the endogenous islets when those are no longer able to maintain normoglycaemia, e.g. in diabetes. At least 75 islets are needed to replace the islets in the pancreas[55]. Secondly, transplanted, vascularized and innervated islets in the ACE can serve as reporter islets to longitudinally and non-invasively study *in vivo* islet morphology[15], β-cell mass and function[56]. This allows cytolabeling *in vivo* to assess cell type and viability *in situ*. Furthermore this approach allows to test the effect of substances or diet interventions on the islets in the living animal as well as real-time tracking of immune cells[57,58]

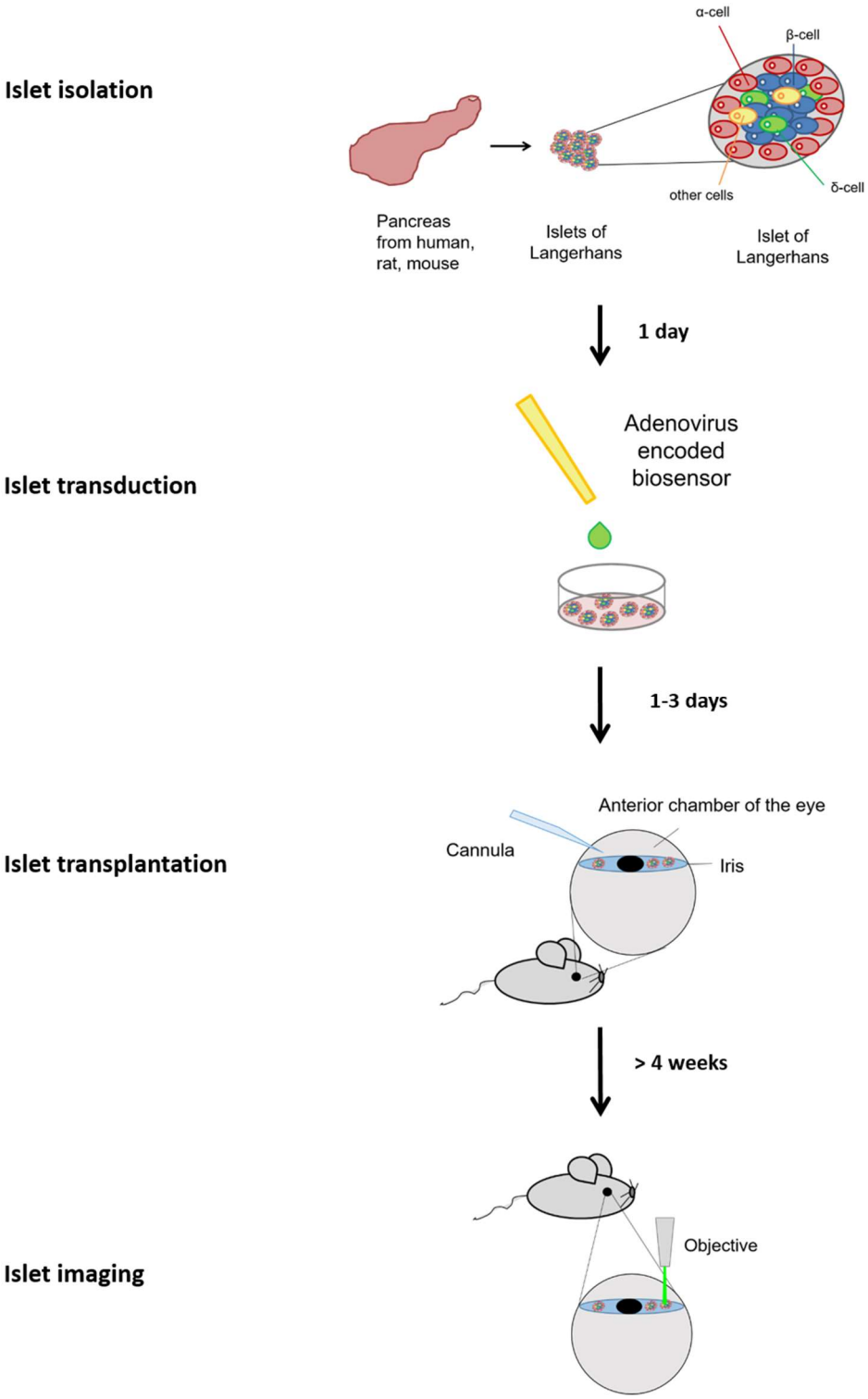

Figure 2.2: The *in vivo* imaging platform

Islets are isolated from recipients by collagenase digestion, followed by handpicking. One day after isolation islets can be transduced by incubation with adenovirus encoding a biosensor. Transduced islets are transplanted into the ACE one to three days after transduction by gently injection through a small hole in the cornea. From four weeks after transplantation islets in the eye can be monitored by microscopy.

2.4 Genetically encoded fluorescent biosensors (GEFBs)

Many different imaging techniques have been employed to study and visualize biological processes and mechanisms in living cells[59]. Outstanding was the development of GEFBs, because their expression can be imaged in living cells without adding exogenous components. Prerequisite for the construction of GEFBs was the discovery of fluorescent proteins. In 1962 Shimomura was the first who extracted and described the green fluorescent protein (GFP) that he found in *Aequorea* jellyfish[60]. Cloning of the gene[61] allowed expression and characterization of GFP in pro- and eukaryotic cells[62]. Chalfie and colleagues realized the potential and advantages of GFP for monitoring of cellular processes in living cells and suggested to use fluorescent proteins as a part of biosensors that report on cellular function. This was beside others done by R. Y. Tsien[63] who also designed different GFP variants such as blue, yellow and cyan fluorescent proteins[64]. During the last 20 years many fluorescent proteins have been developed (overview in [65]) covering today a broad spectrum of colors. Each fluorescent protein has a defined excitation wavelength and a characteristic emission spectrum. This is of particular interest when combining different fluorescent proteins into a single GEFB. The combinatory use of fluorescent proteins requires that they differ in their excitation wavelength and/or emission profile or in the fluorescence life time for distinct identification.

For construction of a GEFB the gene of interest and the cDNA of a fluorescent protein are fused and integrated into an expression construct that is delivered to the target cell by transfection/transduction[16]. In combination with high resolution imaging techniques such as confocal microscopy, subcellular localization as well as translocation of proteins can be monitored. Even co-localization of proteins can be analyzed when different proteins are fluorescently labeled[66]. Driving the expression of a fluorescent protein by a specific promoter allows semi-quantitative analysis of promoter activity[35,67]. Since the copy number of the biosensor can differ from cell to cell and consequently lead to differences in the amount of fluorescence, an internal control is fundamental for semi-quantitative analysis of fluorescence changes. GEFBs can also be used to investigate protein-protein interactions taking advantage of fluorescence/Förster resonance energy transfer (FRET), firstly described in 1948 by Theodor Förster[68] (see also Material and Methods). In general, fluorescent proteins emit fluorescence either permanently or in response to a biochemical stimulus, e.g. pH or Ca^{2+}. Protein interaction also can be studied by linking each part of a split-fluorescent protein to the proteins of interest, generating fluorescence only in case of protein-protein interaction due to protein complementation thus forming an intact fluorescent protein. Many more applications for the use of GEFBs have been described during the last years and are discussed in several reviews[16–18,65].

As mentioned above GEFBs have the advantage that they can be used long-term in living cells/organisms to monitor biological processes. Internal controls allow quantification and the broad spectrum of available fluorescent proteins allows simultaneous observations of different pathways when combining different fluorescent proteins as reporters for different biological processes or readouts (e.g. pH, [ATP], [Ca^{2+}]). In contrast to other methods the biological material needed is relatively low. When using GEFBs, fluorescent proteins have to be chosen carefully considering their fluorescent properties. Validation of results obtained with a new biosensor is indispensable since GEFBs can influence cell function and properties.

3 AIMS

The aims of the thesis were the following:

1. To establish a technique that allows measurements of β-cell insulin sensitivity/resistance longitudinally and non-invasively *in vivo*.
2. To investigate β-cell insulin sensitivity/resistance dynamics in different genetic mouse models of insulin resistance.
3. To explore the relevance of β-cell insulin resistance in diet-induced mouse models of insulin resistance.
4. To start the investigation of the consequences of β-cell insulin resistance for β-cell function.

4 MATERIAL AND METHODS

Cell lines, primary cells, isolated islets of Langerhans as well as mice were used as model systems to establish and validate a method to measure β-cell insulin resistance and to study β-cell insulin resistance in a defined context. They allowed in a simple and time effective way to simulate different situations, e.g. insulin resistance and (pre)diabetes. Using these systems in a stepwise and complexity-increasing way, from cell lines to mouse models, allowed reflection of achieved results before entering the next level. This was especially important when going the step from cell lines to primary cells or islets isolated from animals or humans and even more before performing experiments *in vivo,* to always keep the amount of animals to a minimum and only use them when no other system can be used to answer a particular question. None of the systems will ever have the ability to represent the human situation with its full complexity, but they are useful to test principle ideas and mechanisms under certain situations and contribute to a better understanding of underlying regulation.

4.1 Cell culture

4.1.1 Cell lines

4.1.1.1 MIN6m9 cells

MIN6m9 cells were obtained from Dr. J. Miyazaki[69] and share morphological as well as functional characteristics with mouse pancreatic β-cells, e.g. insulin secretion in response to glucose-stimulation. Therefore they were ideal to investigate molecular mechanisms and to test the basic principle and the regulation of the biosensor. MIN6m9 cells were cultured in Dulbecco´s modified eagles medium (DMEM) supplemented with final concentrations of 11 mM glucose, 75 µM mercaptoethanol, 10% heat inactivated fetal bovine serum (FBS) and 100 U/ml penicillin and 100 µg/ml streptomycin at 5% CO_2 and 37°C.

4.1.1.2 HEK 293A cells

Human embryonic kidney (HEK) 293 cells were generated and established by Graham et al. by transfection of human embryonic kidney cells in 1977 with shared human adenovirus type 5 DNA[70]. The 293A cell line is a subclone of the 293 cell line that has a relatively flat morphology. The genes encoded by the E1 region of adenovirus (E1a and E1b) are expressed in these cells and participate in transactivation of some viral promoters, allowing these cells to produce very high levels of protein. E1 also complements the E1-deletion in recombinant adenoviral vectors, allowing viral replication. In the present thesis HEK 293A cells were exclusively used for adenovirus production. They were cultured in DMEM without pyruvate supplemented with final concentrations of 25 mM glucose, 10% FBS and 1% essential amino acids, but without antibiotics at 5% CO_2 and 37°C.

4.1.2 Islets of Langerhans and primary cells

4.1.2.1 Mouse islets of Langerhans

Mouse islets were used for *in vitro* experiments as well as for transplantation to the ACE of mice. They were obtained from Umeå-ob/ob ($Lep^{ob/ob}$, ob/ob), ob-control ($Lep^{+/+}$, ob-

control), B6 and New Zealand Obese (NZO) mice as described in[14]. Isolated and handpicked islets were cultured in Roswell Park Memorial Institute medium 1640 (RPMI 1640 medium)[71] supplemented with final concentrations of 10% FBS, 2 mM glutamine, 100 U/ml penicillin and 100 µg/ml streptomycin at 5% CO_2 and 37°C.

4.1.2.2 Human islets of Langerhans

Human islets of Langerhans were used to validate findings in the human context. They derived from deceased donors and were isolated at the Division of Clinical Immunology at the University of Uppsala as described in[72]. All experiments were approved by the Regional Ethical Review Boards in Uppsala and Stockholm. Islets were cultured in complete Connaught Medical Research Laboratories (CMRL) 1066 medium supplemented with final concentrations of 11 mM nicotinamide, 2 mM L-glutamine, 5 mM sodium pyruvate, 0.25 µg/ml fungizone, 100 units/ml penicillin G, 100 µg/ml streptomycin-sulfate, 10 mM HEPES, pH 7.4 and 10% FBS at 5% CO_2 and 37°C.

4.1.2.3 Primary cells

To address questions in primary cells, isolated islets were dispersed with Accutase (Innovative Call Technologies, Cytotech, Helleback, Denmark), cells were seeded into 96 well imaging plates and cultured in fully supplemented culture medium.

4.2 Fluorescent biosensors- Construction and use

4.2.1 Fluorescent biosensors

Fluorescent biosensors allow visualization of cellular processes that are otherwise difficult to study (see also Background). Biosensors enable to study certain processes in cells expressing them, but it is possible that the biosensor itself influences the cells. Therefore it is necessary to validate the results obtained with biosensors with independent methods and not exclusively rely on results from biosensors.

4.2.2 Construction of the β-cell insulin resistance biosensor (βIRB)

The adenovirus encoding βIRB was generated as follows: pENTR2A.rat insulin promoter (RIP)1.FoxO1GFP was generated by replacing the cDNA for EGFP in pENTR2A.RIP1.EGFP with that of FoxO1-GFP obtained from pEGFP.N1.hFOXO1[73]. IRES-3Tomato was generated by introducing a cDNA encoding three copies of the red fluorescent protein dTomato[74] downstream of the IRES sequence in pIRES (Clontech, Palo Alto, CA, USA). The IRES-3Tomato cassette was then introduced into pENTR2A.RIP1.FoxO1GFP thus creating pENTR2A.RIP1.FoxO1GFP-IRES-3Tomato. pENTR2A.RIP1.FoxO1(H215R)GFP-IRES-3Tomato was generated by replacing the codon for histidine (CAT) 215 by that of arginine (CGT) by site-directed mutagenesis employing the QuikChange mutagenesis kit (Stratagene, LaJolla, CA, USA) and respective oligonucleotides purchased from Sigma (Paris, France). All constructions were verified by DNA sequencing. The expression cassette was transferred into the promoterless adenovirus plasmid pAd/PL-DEST (Invitrogen, Carlsbad, CA, USA) by the Gateway technique. The ViraPower Adenoviral Expression System (Invitrogen) was used to generate a replication-deficient adenovirus, which was used for the transduction of cells and islets (paper I).

4.2.3 Construction of the β-cell fluorescent metabolic transcriptional response indicator (βFLUOMETRI)

The adenovirus encoding βFLUOMETRI was generated as follows: pENTR1A.RIP1. Red fluorescent protein (DsRed) 2/rbGK.EGFP/ Cytomegalovirus(CMV).Cerulean was generated by inserting the RIP1.DsRed2/rbGK.EGFP-cassette from pd2.RIP1.DsRed2/rbGK.EGFP[75] into pENTR1A (Invitrogen, Carlsbad, CA, USA) and adding a CMV.Cerulean-cassette downstream of the rbGK.EGFP cassette. The three individual expression cassettes are separated by transcription blocker sequences from pd2EGFP-Promoter (Clontech, Palo Alto, CA, USA). The construct was verified by DNA sequencing. The RIP1.DsRed2/rbGK.EGFP/CMV.Cerulean-cassette was transferred into the promoterless adenovirus plasmid pAd/PL-DEST (Invitrogen) by the Gateway technique. The ViraPower Adenoviral Expression System (Invitrogen) was used to generate a replication-deficient adenovirus, which was used for the transduction of islets (paper II).

4.2.4 Adenoviral transduction of cells and islets

Cells and islets (human and mouse) were incubated with 10^7 pfu/ml adenovirus particles encoding the biosensor in fully supplemented medium overnight or for 3.5 hours, respectively. Thereafter the cells and islets were cultured either until *in vitro* experiments or transplantation (only mouse islets!) were carried out.

4.3 *In vitro* experiments with cells and islets of Langerhans

4.3.1 Inhibitor treatment

To investigate the function of a specific protein, the biosensor expressing cells and islets were incubated with an inhibitor or a combination of inhibitors for 1 hour and fixed. Alternatively they were imaged during the incubation with the inhibitor(s).

4.3.2 Antibodies and aptamers

To block the two isoforms of the IR specifically, two blocking antibodies have previously been used, a specific antibody against IR-B and an antibody against both IRs (from Biodesign). Since these antibodies were no longer available and the little difference of only 12 amino acids makes the development of specific (custom made) antibodies difficult, a new method for specific blocking of the two IR isoforms was necessary. DNA-based aptamers, are able to bind their target specifically and inhibit it. The aptamers that selectively recognize and block IRs had been synthesized and produced at POSTECH, Pohang, Republic of Korea using a modified SELEX procedure[76]. For antibody/aptamer treatment, cells were incubated for 30 min with the respective antibodies/aptamers in cell culture medium prior and during the time of EdU incorporation or throughout stimulation with insulin. For insulin stimulation, MIN6 cells were stimulated for up to 10 min with 5 mU/ml insulin in fully supplemented culture medium containing 2 mM glucose.

4.3.3 siRNA-mediated knockdown

Another way to investigate protein function is the application of small interfering (si)RNA. They recognize the corresponding mRNA and silence it by cleavage. For siRNA-mediated knockdown MIN6 cells were first transfected with the siRNA and 48 hours later with other expression constructs of interest for some of the experiments. All experiments were performed between 96 and 120 hours after transfection with the siRNA.

4.3.4 Palmitate preparation and treatment

To simulate a lipotoxic situation, islets were incubated with palmitate. Palmitate was prepared by complexing palmitate (Sigma-Aldrich, St.Louis, MO, USA) with 5% free fatty acid-free BSA[77] and a 0.5% BSA solution was used as control. Transduced islets were incubated in a final concentration of 0.5 mM palmitate or 0.5% BSA in serum free, fully supplemented medium for up to 144 hours.

4.3.5 Measurement of proliferation

Proliferation of cells and islets was measured by using the thymidine analog 5-Ethynyl-2´-deoxyuridine (EdU) that is incorporated into the DNA of dividing cells. The Click-iT EdU Alexa Fluor 488 HCS Assay kit (Invitrogen, Carlsbad, CA, USA) was used to visualize EdU-incorporation. In mouse and human primary islet cell preparations, β-cells were identified by immunostaining with an insulin C-peptide antibody or insulin antibody.

4.3.6 Fixation of cells

For fixation, the cells were grown on coverslips and incubated with 4% Paraformaldehyde in Phosphate-buffered saline solution (PBS) and after washing the coverslips were placed up-side-down on microscope slides with 20 µl embedding medium (4.8% moviol (polyvenyalcohol) and 12% glycerol in Tris HCl-buffer, pH 8.5). Before imaging the embedding medium was allowed to dry for at least 12 hours.

4.4 Animals models for insulin resistance and *in vivo* experiments

4.4.1 Animals

All animal experiments were performed in accordance with the Karolinska Institutet's guidelines for the care and use of animals in research and were approved by the Institute's Animal Ethics Committee. Animals were cage-housed in the animal core facility at Karolinska Hospital at 21°C room temperature at a 12/12 hour day-night-cycle. Before the start of the experiment animals were allowed to acclimatize for at least 1 week.

4.4.1.1 Genetic animal models for insulin resistance

4.4.1.1.1 ob/ob mice

The first description of the obese phenotype of mice, that occurred spontaneous in the V stock at the Jackson laboratory, is from 1950[78]. Genotyping was not developed by that time, but the ob/ob animals could be recognized at an age of 4 to 6 weeks by their body shape. Up to 3 months of age they increase rapidly in body weight which further continues on a lower level throughout their life. Since then, many studies on ob/ob mice were performed to describe and understand their pheno- and genotype more precisely. Batt and Mialhe showed in 1966 that the development of the phenotype was due to the increased food intake. When food intake was restricted to the amount consumed by normal mice, they did not develop high body weight, hyperglycemia and insulin resistance[79]. The leptin gene could be identified as the affected gene, encoding for a hormone that is produced by adipose tissue and responsible for lowering of appetite. Since ob/ob mice cannot produce leptin, food intake is constantly triggered. Consequently leptin injection could restore normal body weight[80,81]. In 1973 Coleman and Hummel showed the importance of the genetic background for the expression of the obese gene in the mouse. The ob/ob mouse is used as model of diabetes, obesity and insulin resistance, but is has to be kept in mind that this model- as other genetic models as well- is in itself only to a minor extend relevant for the human situation where this mutation is rarely found[82].

Leptin deficient ob/ob mice that have been used in the present studies have a C57BL/6J background and are originated from Umeå, Sweden. They were inbred in the animal core facility at Karolinska Hospital. Discrimination between ob/ob and ob-control littermates was achieved by genotype analysis[83]. The ob/ob mice show transient hyperglycemia, hyperlipidemia, hyperinsulinemia, impairment of glucose tolerance, whole-body and β-cell insulin resistance, the islets are increased in number and size[84,85]. The mice improve in some of the parameters as they become older and they do not develop a diabetic phenotype in contrast to ob-mice bred on the C57 BK/KSJ background[86].

4.4.1.1.2 NZO mice (NZO/HlLtJ)

The NZO mice have their origin in the New Zealand Black mouse first described in the 1948 by M. Bielschowsky[87]. They are characterized by high body weight, increased body weight at weaning age and severe obesity in adulthood[88]. Impaired glucose tolerance, increased insulin resistance, hyperinsulinemia, absent rise in plasma insulin levels upon a glucose injection[89] and hyperleptinemia[90] have been described in NZO mice. Both male and female mice have impaired glucose tolerance, but only males develop diabetes (< 50% penetrance)[90] and this was the reason for us to exclusively work with male NZO mice. They have a single point mutation in the gene encoding for the phosphatidlycholine transfer protein, giving the genotype: $Pctp^{R120H}/Pctp^{+}$. The mutation leads to a decrease of phosphatidlycholine transfer activity and abnormal lipid homeostasis[91]. In a publication by Kluth et al. it was shown that carbohydrate-containing diets increase plasma glucose levels in NZO mice. Hyperglycemia leads to dephosphorylating of FoxO1 in the β-cell, which is followed by depletion of insulin stores. β-cell loss is triggered by apoptosis and associated with a reduction in β-cell specific transcription factors[92]. In contrast to the ob/ob mice it has not been described that NZO mice improve their phenotype by age.

Male NZO used in the present studies were purchased from Jackson Labs.

4.4.1.2 Diet-induced animal models for insulin resistance

To come closer to the human situation were a relation between life style, especially eating behavior, weight increase and development of T2DM is seen[1], diet-induced models for insulin resistance were employed. For all diet intervention studies B6 mice (Charles River, Wilmington, MA, USA, male and female) were used. These mice are most commonly used in research, especially for diet intervention studies. B6 mice have been shown to be prone to develop metabolic diseases[39].The following diets were given to 3 months old B6 mice for up to 8 weeks: High Sucrose Diet (HSD): 32% sucrose dissolved in tap water; High Fat Diet (HFD): HFD (60% kcal from fat; Harlan TD.06414); High Fat High Sucrose Diet (HFHSD): HFD + HSD; High Fructose Diet (HFrD): 32% fructose dissolved in tap water; High Fat High Fructose Diet (HFHFrD): HFD + HFrD; Control Diet (Control): Managed formulation purified ingredient diet (Lab Diet; #5P76).

4.4.2 Transplantation of Pancreatic Islets into the ACE

To investigate β-cell insulin resistance and β-cell function *in vivo* the *in vivo* imaging platform (see Background) was used. Here, islets are isolated from mice, transduced with a virus encoding a fluorescent biosensor and then transplanted to the ACE. The *in vivo* imaging platform is used as a model system to monitor islets of Langerhans in the living animal. Since the pancreas can so far not be reached non-invasively with current imaging techniques, it is an attempt to come closer to study the pancreatic islet *in vivo*. Even though the islets are situated in the eye of a living animal, it has to be kept in mind that the location and environment of the islets are different compared to the islets in the endogenous pancreas. Therefore it is necessary to verify results that are obtained by *in vivo* imaging in the eye in the endogenous pancreas.

Transduced donor islets were 1-3 days after transduction transplanted into the ACE of syngeneic, age-matched littermate recipients, using a technique described previously[14,13].

Mice were anesthetized using isoflurane, then a puncture of the cornea was generated with a 27-gauge needle and islets were delivered into the ACE using a glass cannula. Great care was taken to avoid bleeding and damage to the iris. After the transplantation, mice were injected subcutaneously with Temgesic (0.1 ml/kg; Schering-Plough, Kenilworth, NJ) for postoperative analgesia. Before the first imaging islets were let to engraft and vascularize for one month. Re-transplantation to the same or the other eye was performed in two-month intervals if necessary.

4.4.3 *In vivo* measurements and tests in mice

4.4.3.1 Intraperitoneal Glucose Tolerance Test (IPGTT)

Glucose tolerance was measured using the IPGTT where the ability of the body to reduce blood glucose levels within two hours after glucose administration is determined. Mice impaired in glucose tolerance show a more pronounced glucose excursion during the tolerance test than normal mice. The test has the advantage that it is easy to perform and gives fast indications about dysfunction in glucose handling. The disadvantage is that it is a global read-out and not organ-specific.

Mice were fasted for 6 hours during daytime and 2 g glucose (dissolved in PBS)/kg body weight were injected intraperitoneally (i.p.). Glucose levels were determined using the Accu-Chek Aviva monitoring system (Roche, Basel, Switzerland) before the glucose injection and 5 (not always measured), 10, 30, 60 and 120 min after the injection.

4.4.3.2 Intraperitoneal Insulin Tolerance Test (IPITT)

Whole-body insulin resistance was measured employing the IPITT where the ability of the whole body to utilize glucose in the presence of provided insulin is measured. Whole-body insulin resistant mice do not have the ability to use the insulin for glucose uptake. Consequently blood glucose increases more in insulin resistant mice compared to controls where a small increase is followed by relatively stable blood glucose values. This test does not specifically address any specific tissue, but it excludes the involvement of the β-cell since insulin is provided. This experimental setup has the advantage that it is non-invasive and that the animals can undergo the test several times during a long-term study, which was necessary in the present studies. This is also the reason to use the IPITT instead of the euglycemic clamp, where insulin sensitivity of insulin target tissues is measured in a terminal experimental approach[93].

Mice were fasted for 6 hours daytime before the basal glucose state (0 min) was measured. Then, mice were injected with insulin (0.25 U/kg body weight, diluted in PBS, i.p., Novo Nordisk, t = -10 min) followed by glucose administration (1 g/kg body weight, i.p., t = 0 min) and blood glucose concentrations were determined at 15, 30, 60, 90 and 120 min after glucose injection.

4.4.3.3 Pyruvate Tolerance Test (IPPTT)

The ability of the liver to utilize pyruvate and to regulate gluconeogenesis was measured by employing the IPPTT. For this test, low fasting glucose levels are important to address the action of the liver. While normal mice show slightly increased, but otherwise stable blood

glucose, liver insulin insensitive mice do no longer have the ability to regulate gluconeogenesis, resulting in a substantial blood glucose increase. The IPPTT can only be seen in the context of other measurements and tests.

To achieve sufficient low glucose levels mice were fasted for 12 hours over night and blood glucose was measured at basal state (0 min). 2 g pyruvate (dissolved in PBS)/kg body weight were injected i.p. and blood glucose levels were determined 30, 60, 90, 120 and 180 min after the injection.

4.4.3.4 Body weight and fasting blood glucose

Body weight and fasting blood glucose were measured after 6 hours fasting time.

4.4.3.5 Serum biochemistry

To analyze factors in the serum, blood samples were obtained at all time points during the IPGTT, centrifuged to obtain blood serum and preserved at −20°C until measurement. Ultrasensitive mouse enzyme-linked immunosorbent assay (ELISA) kits (CrystalChem, Zaandam, Netherlands) were used to analyze different factors in the serum, e.g. C-peptide and insulin.

4.5 Imaging and image analysis

4.5.1 *In vitro* imaging

4.5.1.1 *In vitro* imaging of cells

Either living or fixed cells were imaged using a laser-scanning microscope from Leica Microsystems, Germany (Leica TCS SP2). A central plane of each cell was imaged. An objective with the following settings was used for detection: Leica HCX PL APO 63x/1.20 NA. Excitation wavelengths and detection ranges were chosen in respect to the particular fluorescent proteins. For more details please see the method section of the corresponding paper.

4.5.1.2 FRET analysis by acceptor photobleaching

FRET analysis by acceptor photobleaching was used to measure protein/protein interactions. The method described by Karpova and McNally was adapted to the Leica TCS-SP2 confocal microscope[94]. To determine FRET between IR-B (acceptor) and PI3K-C2α or Shc (donors) cells were transfected with constructs encoding mCerulean- or mCyan Fluorescent Protein (CFP)- (donor) and mVenus-(acceptor) tagged proteins and fixed before the experiment. As illustrated in Fig. 4.1A in total 3 images were obtained with the following settings: mCerulean or mCFP: Excitation 458 nm (laser-power 15%), emission detection at 470-490 nm; mVenus: emission detection at 520-550 nm. Image 1 and 2 were obtained 1 min part from each other, image 3 was taken after photobleaching of the FRET-acceptor mVenus for 1 min by excitation with the 514 nm laser at full power. The values for FRET transfer efficiency E_F and control FRET transfer efficiency C_F and were calculated using the following formulas and having CFP-intensity (CFP) as signal for either mCFP or mCerulean: $C_F=(CFP_2 - CFP_1)/CFP_1$; $E_F=(CFP_3–CFP_2)/CFP_2$. All intensities were background-corrected before respective calculations. FRET did occur if E_F was significantly higher than C_F, reflecting that photobleaching of the FRET-acceptor mVenus would lead to an increased emission of the FRET-donors mCerulean or mCFP (Fig. 4.1B).

4.5.1.3 *In vitro* imaging of islets of Langerhans

Islets were imaged *in vitro* using a laser-scanning microscope from Leica Microsystems, Germany (Leica TCS SP2). Images were obtained as 3D-stacks with a step-size of 2 µm using a Leica HCX PL APO 20x/0.7 NA. Excitation wavelengths and detection ranges were chosen in respect to the particular fluorescent proteins. For more details please see the method section of the corresponding paper.

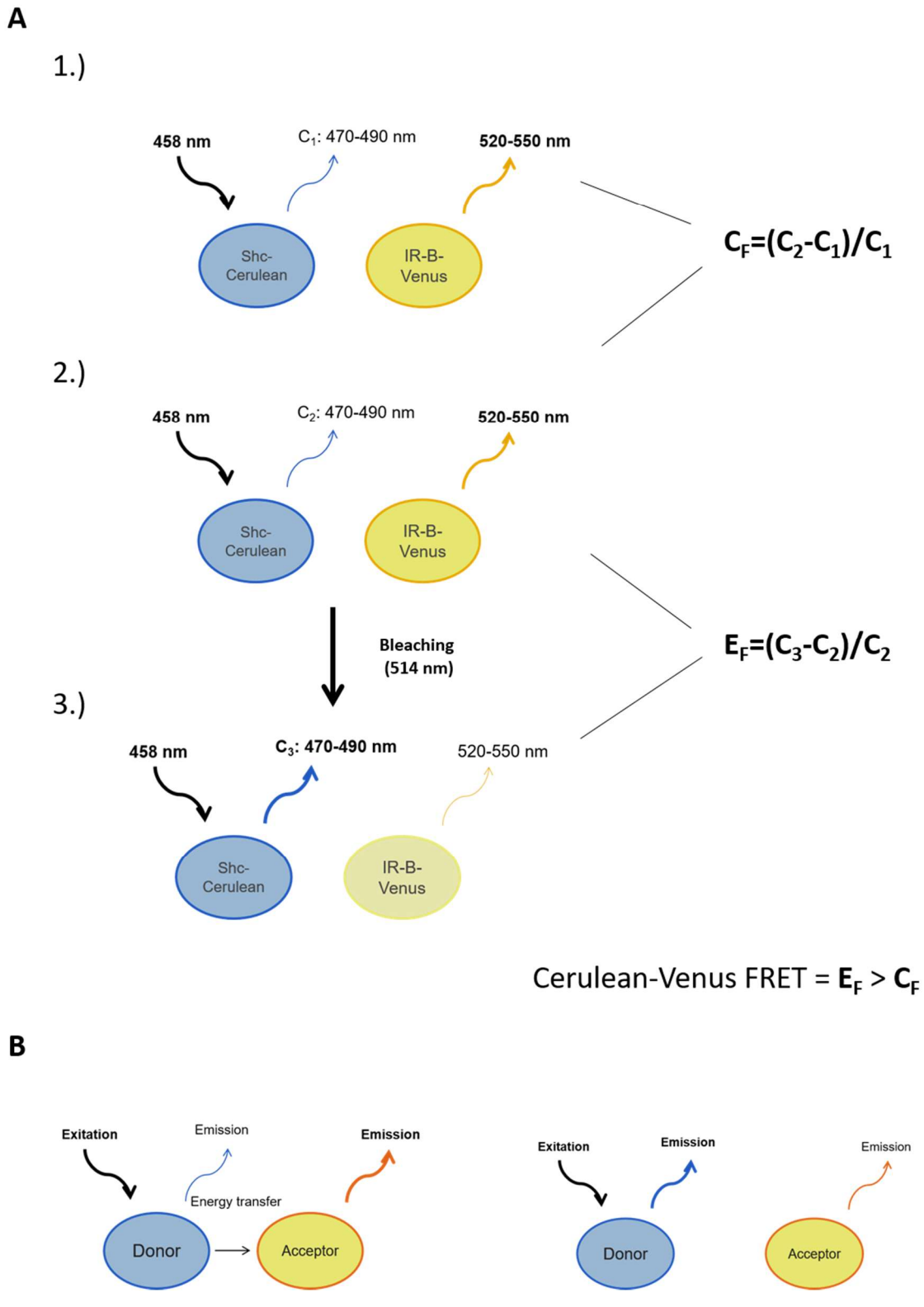

Fig. 4.1: FRET analysis by acceptor photobleaching
(A) Donor emission is measured twice (1., 2.) one minute apart from each other and C_F is calculated. After acceptor bleaching donor emission is measured a third time (3.), used to calculate E_F. (B) When $E_F > C_F$, FRET occurred and both fluorophores are in close proximity to each other.

4.5.2 *In vivo* imaging

4.5.2.1 *In vivo* imaging of islets in the ACE

Transduced and transplanted islets were regularly imaged from 1 month after transplantation on[14,13]. Mice were anesthetized with isoflurane and the islets in the mouse eye were kept in a static position during imaging by a custom-built stereotaxic head holder. For the imaging Viscotears (Novartis, Basel, Switzerland) was administered as an immersion liquid between the eye and the objective. An upright laser scanning confocal microscope (Leica TCS SP5, LEICA Microsystems, Wetzlar, Germany) equipped with a long-distance water-dipping objective (Leica HXC-APO 10×/0.30 NA) was used. Excitation wavelengths and detection ranges were chosen in respect to the particular fluorescent proteins. In addition the backscatter signal from the 561 nm excitation was always collected at 555 to 565 nm[56]. For more details, please see the method section of the corresponding paper.

4.5.2.2 *In vivo* Ca^{2+} imaging

For calcium measurements islets from male B6 mice, heterozygous for InsCRE and floxed GCaMP3[95,96] were isolated and used for transplantation. From 4 weeks after transplantation on imaging was performed as follows: 4 hours fasted mice were anesthetized with midazolam/fentanyl/fluanison (i.p.) and during the imaging supplied with oxygen via a nose mask. The whole microscope was enclosed and heated to 35°C and a 25x/0.95 NA objective was used. GCaMP3 was excited with 488 nm and fluorescence was detected at 500-550 nm. A tail vein catheter containing 14 µl Heparin (100 IE)/ml was inserted in the mouse´s tail and Heparin was injected. 2 minutes after the start of the imaging glucose (0.4 g/kg) was carefully injected into the catheter. Images were acquired with µManager over a time of 20 min after glucose application[97].

4.5.3 Image analysis

4.5.3.1 Analysis of the β-cell insulin resistance biosensor

To analyze FoxO1 distribution in the cell, i.e. the insulin sensitivity status of the cell, unbiased analysis of images obtained by *in vitro* or *in vivo* imaging of cells and islets of Langerhans was done with the Leica LAS software. Here, the central plane of each cell was determined using information from the three detection channels (GFP, Tomato, and backscatter). To calculate the ratio of nuclear FoxO1 ($FoxO1_{nuc}$) to cytoplasmic FoxO1 ($FoxO1_{cyt}$), fluorescence intensities of the GFP channel were obtained within three regions of interest (nucleus, cytoplasm and background (BG)) that were manually drawn for each cell. For each cell a ratio was calculated based on the obtained fluorescence intensity values: ratio $r = (FoxO1_{nuc}\text{-}BG)/(FoxO1_{cyt}\text{-}BG)$. For each experimental *in vitro* and *in vivo* condition the ratio was calculated. In the first set of experiments (paper I), cells with a ratio $r \geq 1$ were categorized as insulin resistant and cells with a ratio $r < 1$ as insulin responsive. Then a percentage of insulin resistant cells was calculated and used for statistical analysis.

Since it was not known whether $FoxO1_{nuc} \geq FoxO1_{cyt}$ had to be fulfilled for insulin resistance and even an increase in the ratio towards more $FoxO1_{nuc}$ could be relevant, in following experiments the normalized ratio was used for comparison and statistical analysis (paper II). To normalize the ratio a correction value c was used to calculate the relative β-cell insulin resistance index (rβIRI) for each time point and experimental group: $r\beta IRI = r/c$.

For *in vivo* experiments, the mean ratio of the experimental starting time point (t=0) and/or control group was used as correction value. More precisely, in the genetic animal studies the mean ratio of ob-control mice at 3 months of age was used as correction value. In the diet intervention study, the mean ratio of all mice at the time point before the treatment was used as correction value. The rβIRI was considered a measure of β-cell insulin resistance and used for further statistical analysis. For *in vitro* experiments, the mean ratio of the control group for each individual time point (correction value c) was used to further calculate the rβIRI for each time point and experimental group: rβIRI = r/c. All images were analyzed using Leica LAS software (Leica Microsystems, Wetzlar, Germany).

4.5.3.2 Analysis of βFLUORIMETRI

To calculate the change in fluorescence after glucose stimulation as a readout of β-cell functionality, fluorescence intensities for each cell were determined at the beginning of the experiment and 4 hours after glucose stimulation. Cells were identified using the DsRed-fluorescence signal thereby ensuring the analysis of β-cells. Promoter activation was calculated as follows:
$((GFP/DsRed_{240min}\text{-}Background_{240min}) / (CFP_{240min}\text{-}Background_{240min})) / ((GFP/DsRed_{Start}\text{-}Background_{Start}) / (CFP_{Start}\text{-}Background_{Start}))$.
To determine functional β-cell mass as % of glucose responsive cells, cells with a promoter activation >1.15 were considered responsive.

Image analysis for *in vitro* experiments was performed as described in ([35,67,98,99]) using ImageJ. Average fluorescence intensities for each cell were determined for t = 60 min (start) and t = 240 min.

Images derived from *in vivo* imaging were analyzed using Leica LAS software (Leica Microsystems, Wetzlar, Germany). For each analyzed cell, fluorescence intensity for all three fluorescent dyes (CFP, GFP, DsRed) was determined before glucose stimulation and 240 minutes after glucose stimulation.

4.5.3.3 Backscatter intensity

Backscatter intensity was used as indicator for insulin content as described in[56] and was analyzed in the backscatter images obtained during the imaging of βFLUOMETRI-biosensor using ImageJ. Average signal intensity of the islet was normalized to average signal intensity of the surrounding iris and the ratio was used as backscatter intensity (A.U.).

4.5.3.4 Islet size

Islet size was determined based on the backscatter images obtained during the imaging of the βFLUOMETRI-biosensor as described in[100] using ImageJ. Islet volume was extrapolated from maximum projected area and z-depth. Relative islet size was calculated by dividing the islet size at 8 weeks by islet size at the start of the experiment for each individual islet.

4.5.3.5 Analysis of calcium imaging

Image processing was done in Matlab (The MathWorks, USA). Every z-stack was denoised[101] and consecutive planes were aligned[102]. Z-stacks were deconvolved[103] and

registered to a reference z-stack[104]. Individual β-cells were identified based on their temporal $[Ca^{2+}]_i$ profile. Single cell $[Ca^{2+}]_i$ traces were normalized to their baseline. β-cells were considered responding when their glucose induced $[Ca^{2+}]_i$ increase was larger than three times the standard deviation before glucose injection.

4.6 *Ex vivo* analysis of pancreas tissue and islets of Langerhans

4.6.1 *In situ* analysis of pancreas tissue

4.6.1.1 Pancreas extraction and sectioning

Pancreas tissue was obtained and sectioned to verify and complement data obtained *in vivo*. Mice were anesthetized with isoflurane and transcardially perfused with PBS followed by freshly prepared 4% (wt/vol) paraformaldehyde in PBS. Pancreas were dissected and post-fixed for 2 hours. Prior to cryopreservation the tissues were processed with a sucrose gradient [10-30% (wt/vol) sucrose in PBS containing 0.01% (wt/vol) sodium azide and 0.02% (wt/vol) bacitracin], then frozen in dry ice and preserved at −80 °C until use. 20 µm thick pancreas cryosections were collected on SuperFrost Plus microscope slides (VWR) and kept at -20°C until use.

4.6.1.2 Immunofluorescence in pancreas tissue

For immunostaining, pancreas tissue cryosections were equilibrated to room temperature, washed, blocked and then incubated with the primary antibodies in the presence of 0.1% Triton-X100 and 10% FBS at 4°C. After washing, secondary antibodies were applied at 4°C and mounting with medium containing DAPI for nuclear counterstaining (Life Technologies) was performed after repeated washing. Images were captured using the Pathway 855 imaging system (BD Biosciences, San Jose, CA, USA) and analyzed using ImageJ. Please see corresponding papers for specific information on used antibodies.

4.6.1.3 β-cell proliferation measurement with BrdU

To assess β-cell proliferation *in vivo*, 0.8 mg/ml of the synthetic nucleoside and thymidine analog BrdU (Life Technologies, Carlsbad, CA, USA) was added to the drinking water of the mice for one week during the second month of diet intervention. After isolation and sectioning, pancreas were stained for BrdU and insulin to determine the amount of proliferating β-cells.

The images were obtained with the Pathway 855 imaging system (BD Biosciences, San Jose, CA, USA) and were analyzed with the Cell Profiler (http://cellprofiler.org/). Nuclei were identified by 4',6-diamidino-2-phenylindole (DAPI) staining; the intensities of the insulin and BrdU staining were measured in nuclear regions and displayed as histogram. Insulin positive objects were defined as β-cells. BrdU-positive and –negative cells were identified and used for calculation of the percentage of BrdU-positive β-cells and statistical analysis.

4.6.2 *In vitro* analysis of islets of Langerhans

4.6.2.1 Immunofluorescence in isolated islets of Langerhans

Immunofluorescence of pancreatic endogenous FoxO1 localization in isolated islets of Langerhans was performed to verify the data from *in vivo* imaging. Briefly, freshly isolated islets were fixed with 4% paraformaldehyde in PBS for at least 48 hours at 4°C. Islets were incubated with primary antibodies (anti-FoxO1, anti-insulin) in the presence of 0.5% Triton-X100 for permeabilization and 10% FBS or 2% of BSA for blocking at 4°C. After removing

the primary antibodies and repeated washing with PBS, secondary antibodies were applied at 4°C. The islets were imaged by confocal laser scanning microscopy after repeated washing. Since collagenase digestion during the islet isolation carries the risk of islet damage and the time between islet isolation and staining can change the islet compared to the actual *in vivo* situation, these results were confirmed by *in situ* immunofluorescence staining of pancreas tissue sections that were obtained from pancreas isolated after perfusion of the animals.

4.6.2.2 Western Blotting analysis of islets of Langerhans

Western blotting was used to specifically quantify proteins and protein phosphorylation. On the one hand, it was used to verify the data obtained by *in vivo* imaging of FoxO1 and on the other hand to characterize the status of a β-cell insulin resistant islet cell. Islets were lysed immediately after isolation in lysis buffer (50 mM Tris (pH 7.5), 1 mM EDTA, 1 mM EGTA, 0.5 mM Na3VO4, 0.1% (v/v) 2- mercaptoethanol, 1% Triton X-100, 50 mM NaF, 5 nM sodium pyrophosphate, 10 mM sodium β-glycerol phosphate, 0.1 mM PMSF, 1 µM Microcystin, 1 µg/ml of aprotinin, pepstatine and leupeptin each). The proteins (45 µg) were separated over a 7.5% SDS-polyacrylamide gel (buffering system according to Laemmli) and electrotransferred to Polyvinylidenedifluoride membrane. In case of phospho-specific antibodies the membranes were probed first with the respective phospho-specific antibodies, then stripped and re-probed with antibodies recognizing the respective total protein levels. Please see publications for specific information on used antibodies. Immunoreactivity was detected with horseradish peroxidase-conjugated secondary antibodies using Clarity Western ECL Substrate and the Chemi Doc Touch Imaging System (BioRad, Hercules, California, USA). Band intensities were quantified using Image Lab 5.2.1 software from BioRad.

4.6.2.3 (Co-) Immunoprecipitation

(Co-) Immunoprecipitation was used for analysis of IR-B and Shc interaction in MIN6m9 cells as well as interaction of IR-B and Shc or p85 in islets of ob/ob mice.
Cells were lysed in co-immunoprecipitation lysis buffer (20 mM Tris-HCl pH 8.0, 137 mM NaCl, 15% glycerol, 0.5% Triton X-100, 1 mM PMSF, 10 mM NaF, 4 mM Na3VO4, 1 µg/ml aprotinin, leupeptin and pepstatin each). The lysate was incubated for 30 min at 4°C on a rotator, centrifuged (15 min at 12 000 x g) and the supernatant was collected. 1 mg of protein was incubated with 5 µg of the immunoprecipitation antibody on a rotator for 16 hours at 4°C. 50 µl of pre-eliquibrated protein A/G Plus agarose (Santa Cruz Biotechnology, USA) were added and incubated for additional 4 hours. Immunoprecipitates were washed three times with lysis buffer on ice and then resuspended in 2x SDS sample buffer, boiled and separated on a SDS-polyacrylamide gel. Western blot analysis was performed with the respective antibodies.
For the IR-B/Shc interaction experiment MIN6m9 cells were co-transfected with control siRNA or siRNA against PI3K-C2α and myc-tagged IR-B. 96 hours after start of transfection cells were starved for 6 hours in fully-supplemented culture medium containing 2 mM glucose. After stimulation with insulin (5 mU/ml) for 10 min cells were lysed. Interaction of myc-tagged IR-B with Shc was analyzed with Shc antibody in myc-antibody immunoprecipitates.

For the co-immunoprecipitation analysis in ob/ob islets, islets from 9-10 mice were pooled and disrupted immediately after isolation by treatment with Accutase (Innovative Cell Technologies) prior to lysis. IRs were immunoprecipitated and blotted. The membranes were probed with the following antibodies: rabbit monoclonal PI3 Kinase p85 antibody, rabbit monoclonal IR β antibody or mouse monoclonal IR β antibody, rabbit polyclonal Shc antibody (all from Cell Signaling Technology) or mouse monoclonal Shc antibody (BD Transduction Laboratories).

4.6.2.4 Gene expression analysis of islets of Langerhans

Gene expression analysis of certain genes was used to investigate the molecular consequences of β-cell insulin resistance on the β-cell. 100-200 freshly isolated islets were processed with RNeasy Mini Kit (Qiagen, Venlo, Netherlands) to isolate RNA. cDNA was synthesized using RT^2 First Strand Kit and used in a SYBR Green based custom PCR array (Qiagen). Analysis was performed as described elsewhere[105], where the $2^{-\Delta CT}$ was calculated for experimental groups and used for further statistical analysis.

4.7 Data presentation and statistics

Origin 2015 64 Bit and Microsoft Office EXCEL were used for statistical analysis. The values are expressed as mean ± S.E.M.. The two-sided, unpaired t-test was used to determine statistical significance between experimental groups and the two-sided, paired t-test was used for comparison within the same experimental group at different time points of the study. Data were checked for outliers using Grubbs´ test. Statistical significance was defined as follows: $*p < 0.05$, $**p < 0.01$ and $***p < 0.001$. The data were graphically illustrated using Origin 2015 64 Bit.

5 RESULTS AND DISCUSSION

5.1 A method to measure β-cell insulin sensitivity/resistance *in vivo*

To establish a technique to monitor β-cell insulin sensitivity/resistance *in vivo* at the single cell level longitudinally and non-invasively we used the *in vivo* imaging platform (see Background). To distinguish insulin responsive from insulin resistant β-cells we designed a genetically encoded fluorescent biosensor (GEFB) that is expressed in β-cells. Pancreatic islets, prior to their transplantation into the ACE, were transduced with an adenovirus encoding the biosensor.

5.1.1 Concept and design of β-cell insulin resistance biosensor (βIRB)

For the development of the biosensor we took advantage of the ability of the transcription factor FoxO1 to change its localization within the cell in response to insulin resistance. Under insulin responsive (normal) conditions FoxO1 is phosphorylated by the serine/threonine kinase Akt preventing its nuclear import and resulting in cytosolic localization. In a situation of insulin resistance, Akt is no longer able to phosphorylate FoxO1 which results in FoxO1 shuttling into the nucleus (Fig. 5.1. A) [73,106,107].

For detection by confocal fluorescent microscopy we fused GFP to FoxO1. To minimize the influence of the biosensor on cell function, we mutated the DNA-binding site of FoxO1 to disallow its DNA binding and avoid its function as a transcription factor, resulting in FoxO1(H215R)[108]. Since the remaining parts of FoxO1 were unchanged, it was comparable to endogenous FoxO1. We additionally introduced into the biosensor a triple Tomato cDNA (3Tomato) which was separated from the FoxO1-GFP cassette by a virus-derived IRES-element, allowing co-expression of FoxO1-GFP and 3Tomato. 3Tomato was originally intended to be used as a topological and ratiometric reference. It has a total molecular weight of 81 kDa and should therefore stay in the cytoplasm and not diffuse into the nucleus, because the nuclear pore complex allows passive import of molecules with a maximal size of 60 kDa. However, 3Tomato was detectable in the nucleus and had reached the nucleus by a yet unknown mechanism. Nevertheless, 3Tomato served for identification of cells expressing the biosensor. To ensure β-cell specific expression of the biosensor we choose the RIP1 (-410/+1bp) (paper I, fig. 1a). The hypothetical expectation that FoxO1(H215)GFP is detectable in the cytoplasm in the insulin-responsive situation and in the nucleus in the case of insulin resistance is schematically illustrated in Figure 5.1. B.

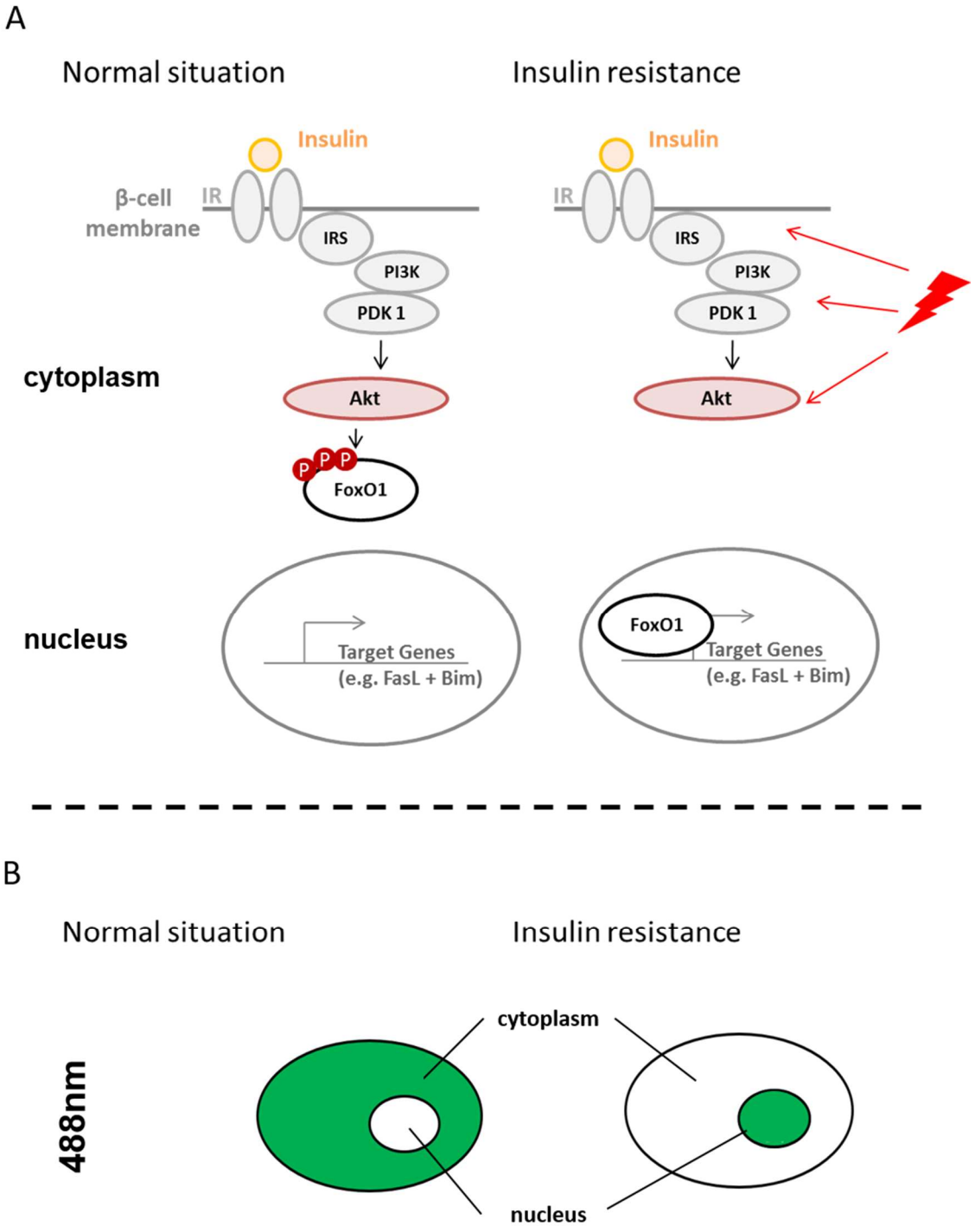

Figure 5.1: FoxO1 localization under normal and insulin resistance conditions

(A) If insulin signaling downstream of the insulin receptor is functional, FoxO1 is phosphorylated by Akt and stays in the cytoplasm. In case the insulin signaling cascade is non-functional, FoxO1 is no longer phosphorylated by Akt and shuttles into the nucleus. The cell is in a state of insulin resistance. (B) Schematic illustration of the working principle of βIRB. Adenoviruses encoding βIRB are used to transduce MIN6 cells and pancreatic islets. The fluorescent indicator GFP is identified by laser-scanning fluorescent confocal microscopy upon excitation with 488 nm. Under normal conditions FoxO1(H215R)GFP (green) is cytoplasmic and it shuttles into the nucleus at insulin resistance.

5.1.2 βIRB can be used for *in vitro* assessment of β-cell insulin sensitivity/resistance

To verify the function and the concept of the biosensor we transduced MIN6 cells and mouse islets of Langerhans with adenoviruses encoding βIRB and incubated some of the cells and islets with the Akt-inhibitor Akti-1/2, thus mimicking insulin resistance. As shown in paper I, fig. 2a, b and 3b FoxO1(H215R)GFP was present in the cytoplasm under normal culture conditions and was located in the nucleus when incubated with the Akt inhibitor. In addition, we mimicked lipotoxic conditions by incubating mouse and human islets with palmitate. Also under these conditions the biosensor indicated insulin resistance (paper I, fig. 3f-k). β-cell specific expression was tested by immunostaining for insulin in transduced islets of Langerhans. As fig. 3a in paper I shows, only β-cells were expressing the biosensor. This demonstrated that the biosensor worked as intended.

5.1.3 βIRB indicates β-cell insulin resistance in insulin receptor and Akt-dependent signaling

Insulin signaling in the β-cell is complex and many different insulin signaling cascades co-exist (reviewed in [6]). It is well accepted that Akt serves as a central player in the metabolic branch of insulin signaling. Thus, we defined insulin resistance in the β-cell as any possible disturbance in insulin signaling that impairs Akt activity (Fig. 5.1 A). The first step was to test the involvement of IRs and/or insulin like growth factor 1 (IGF-1) receptor in the signal transduction to βIRB. For that purpose we incubated MIN6 cells and mouse islets of Langerhans with $HNMPA(AM)_3$, (100 μM, for 1 hour) an universal IR inhibitor, or the IGF-1 receptor inhibitor PPP (2.4 μM, for 1 hour). The results revealed that only blocking of IRs led to a change in location of FoxO1(HR)GFP, but not the inhibition of the IGF-1 receptor (paper I, fig. 2e and 3c-e). This clearly showed that βIRB nuclear exclusion is IR-dependent, but not dependent on IGF-1 receptor signaling. These results are in agreement with data from IR and IGF-1 receptor KO mice, demonstrating that insulin signaling downstream of the IR, but not IGF-1 receptor, is important for FoxO1 nucleus exclusion in the β-cell[11].

In MIN6 cells all three isoforms of Akt, i.e. Akt1-3, are expressed[99]. We next examined which isoform of Akt is responsible for regulation of βIRB. We employed the Akt inhibitors 1/2 (Akti-1/2) (0.1 to 10 μM, for 1h), inhibiting the three isoforms at different concentrations (IC_{50}= 58 nM, 210 nM, and 2.12 μM *in vitro* for Akt1, Akt2 and Akt3, respectively) and an Akt-2 isoform selective inhibitor (Akti-2) (4 μM, for 1h). The results showed that all three isoforms convey the signal leading to biosensor location (paper I, fig. 2b-d). Consequently, our data confirmed that βIRB reports on β-cell insulin sensitivity that reflects IR/Akt-dependent signaling. This was further supported by Western blot analysis of islets from βIRB-indicated β-cell insulin resistant mice fed a HFHSD for 8 weeks. In these islets tyrosine phosphorylation of the IR at Tyr-1150/1151, Akt phosphorylation at Ser-473 and FoxO1 phosphorylation at Ser-256 were decreased (paper II, fig. 2c-e).

5.1.4 βIRB can be used for *in vivo* assessment of β-cell insulin resistance

The main goal of generating βIRB was the investigation of β-cell insulin sensitivity *in vivo* by using the *in vivo* imaging technique (see Background). To test the biosensor *in vivo*, we employed the leptin-deficient ob/ob mouse, because the phenotype of this mouse is well characterized. The ob/ob mouse is described as transient hyperglycemic, hyperinsulinemic, whole-body and β-cell insulin resistant and shows impaired glucose tolerance at young age which improves later in life (see Material and Methods)[84,85]. βIRB expressing islets were

transplanted into the ACE of age-matched littermates. Since ob/ob mice were whole-body insulin resistant at young age (3 months) and showed improved insulin sensitivity at older age (10 months) (paper I, fig. 4a, b), we chose these two time points to test the biosensor. Our results indicated that also the β-cell is insulin resistant at 3 months of age while it is insulin responsive at 10 months of age (paper I, fig. 4c, d). To verify these results we isolated islets from animals at these respective ages. Immunostaining showed also significantly more endogenous FoxO1 in the nuclei of β-cells from young ob/ob mice compared to young ob-control mice and old ob/ob mice (paper I, fig. 4e, f). Western blot analysis of the pFoxO1/FoxO1 ratio confirmed that less FoxO1 is phosphorylated in young compared to old ob/ob mice (paper I, fig. 4g). These data demonstrated that the βIRB can be used to measure β-cell insulin sensitivity *in vivo*.

5.1.5 The fluorescence intensity of the βIRB decreases time-dependently

The biosensor was intended to be used longitudinally *in vivo*, however, our data showed that the amount of analyzable βIRB-expressing cells decreased with time (paper I, fig. S1). We overcame this problem by re-transplanting the mice with freshly isolated and transduced islets from littermates or age-matched mice every second month. Thus, we were able to monitor the same animal up to 8 months after transplantation, but not the same islets and accordingly cells. The decline of analyzable cells was due to a time-dependent reduction in fluorescence and independent of imaging (Fig. 5.2). This is most probably due to enforced degradation of the biosensor. Since the decline of detectable cells is not universal for all adenovirus encoded biosensors (see βFLUOMETRI), the rapid decrease in expression due to adenoviral transgene degradation can be disregarded at this point. The whole problem of decrease in amount of analyzable cells could be overcome by the generation of a genetically modified mouse that expresses FoxO1(HR)GFP in its β-cells. There all β-cells would permanently express FoxO1(HR)GFP and the amount of FoxO1(HR)GFP-positive cells would be much higher than in islets transduced with the adenovirus. This has successfully been shown in GCaMP3-mice ([109], S. Jacob et al.; unpublished data).

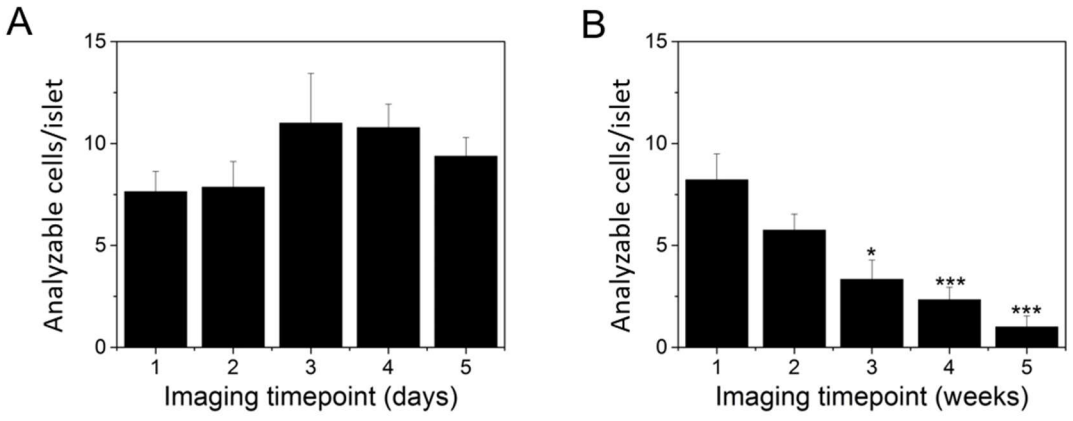

Figure 5.2: *In vitro* assessment of the decline of analyzable cells

Isolated islets were transduced with adenoviruses encoding βIRB and imaged either daily (A) or weekly (B). In these islets the amount of analyzable fluorescent cells per islet was determined.

5.2 β-cell insulin resistance in genetic mouse models

5.2.1 β-cell insulin resistance in ob/ob mice changes over time

We continued to use βIRB in leptin deficient ob/ob mice to investigate the dynamics of β-cell insulin resistance longitudinally from 3 to 10 months of age. To additionally assess the dynamics of the onset of β-cell insulins resistance during month 1 and 2, we needed to perform immunostaining of endogenous FoxO1 in isolated islets at these time points, because it was technically not possible to transplant mice with biosensor expressing reporter islets before the age of 2 months. Since we have previously shown (paper I) that immunostaining of endogenous FoxO1 and *in vivo* imaging of βIRB gave the same results, we were confident to combine these two techniques to investigate β-cell insulin resistance over time. To minimize the amount of animals, monitoring of βIRB by *in vivo* imaging was the preferred method for this study and used when possible. We combined β-cell insulin resistance monitoring with physiological measurements of whole-body and liver insulin resistance, glucose tolerance and body weight. The results (Fig. 5.3 A-D) showed that ob/ob mice developed β-cell insulin resistance together with whole-body and liver insulin resistance as well as impaired glucose tolerance during their second month of life. Furthermore, we could demonstrate that β-cell insulin resistance was the first to recover before glucose tolerance, whole-body and liver insulin resistance normalized. This approach was not sufficient to indicate whether β-cell insulin sensitivity is the cause or the consequence of impaired glucose and insulin tolerance, but obviously β-cell insulin resistance can improve independently of still present impairment in the other physiological parameters.

Only the body weight remained increased throughout the study, but the strongest body weight increase was seen within in the first three months (Fig. 5.3 E). In ob/ob mice β-cell insulin resistance was present in a phase of life of rapid and extensive body weight increase, where impaired glucose, whole-body and liver insulin tolerance were at their maximum. To validate a possible function of β-cell insulin resistance in ob/ob mice during this period of life, in-depth analysis of β-cells at this specific time points has to be performed.

In general these results demonstrated that β-cell insulin resistance can be a temporary state. The molecular mechanisms underlying β-cell insulin resistance as well as functional consequences should be addressed in the future.

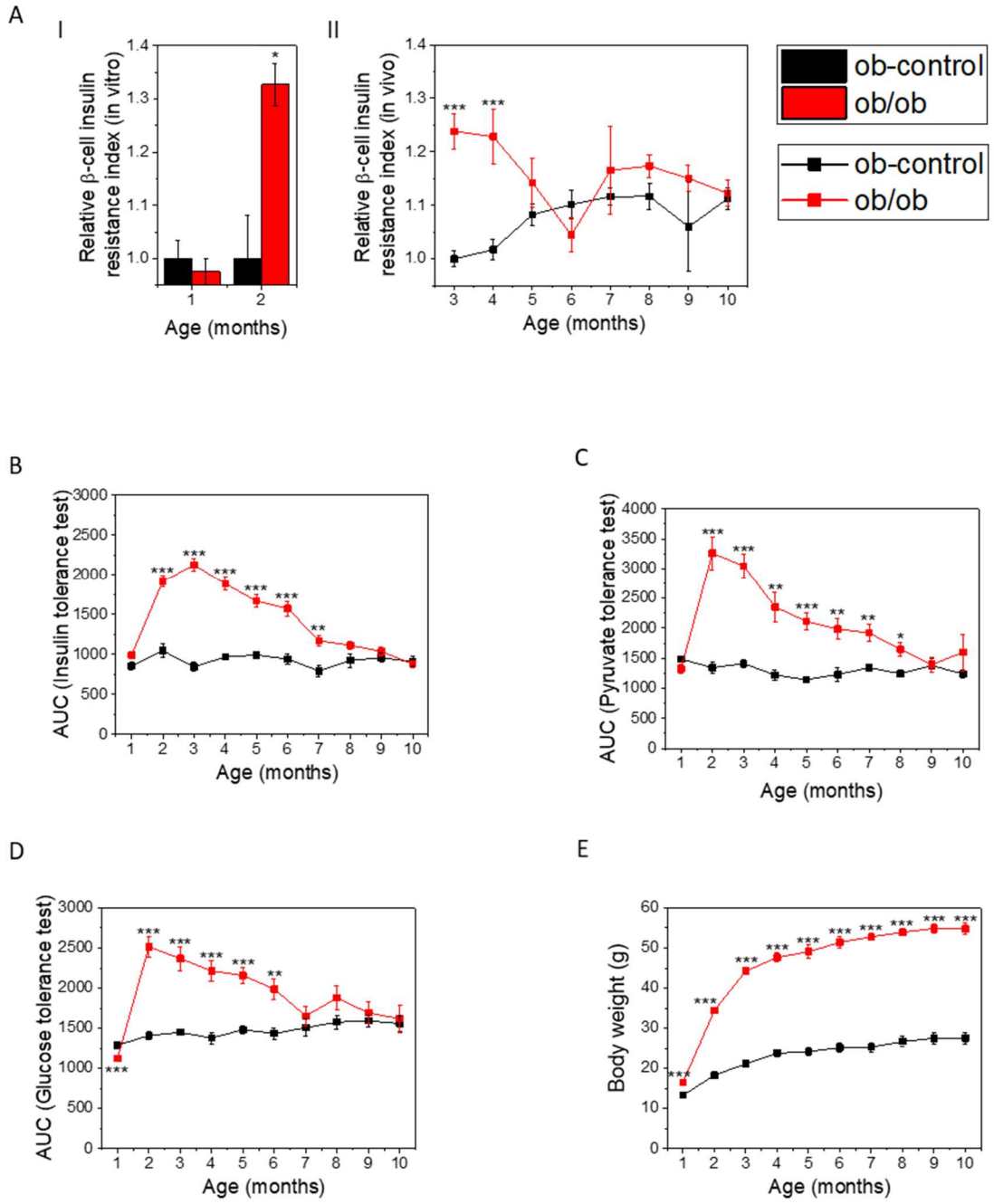

Figure 5.3: Dynamics of insulin resistance and other physiological parameters obtained in ob/ob mice

(A) β-cell insulin resistance: (I) Relative β-cell insulin resistance index calculated from the subcellular distribution of endogenous FoxO1 in *in situ* islets obtained from the pancreas of ob/ob and ob-control mice at 1 and 2 months of age. (n=4-5 mice) (II) Relative β-cell insulin resistance index of ob-control and ob/ob mice from 3 to 10 months of age obtained with βIRB (n=12-15). (B) Whole-body insulin resistance obtained by the IPITT and depicted as area under the curve (AUC) of the individual traces obtained during the IPITT (n=3-12). (C) Liver insulin resistance obtained by the IPPTT and depicted as AUC of the individual traces of the IPPTT (n=3-9). (D) Glucose tolerance obtained by the IPGTT and depicted as AUC of the individual traces obtained during the IPGTT (n=4-14). (E) Body weight (n=16).

(A-E) All studies have been conducted with ob/ob and ob-control mice from 1 to 10 months of age. *p<0.05; **p<0.01; ***p < 0.001. Data are expressed as mean ± SEM.

5.2.2 β-cell insulin resistance has different dynamics in NZO mice

To address the question whether insulin resistance dynamics are similar in different mouse models, we employed NZO mice (see Material and Methods) to obtain the same physiological parameters as in ob/ob mice. These mice have been shown to develop severe obesity and T2DM. Furthermore, dephosphorylation of FoxO1 caused by hyperglycemia was demonstrated in their β-cells[92]. Since an appropriate control for NZO mice was not available, we used ob/ob and ob-control mice for comparison. As Fig. 5.4 shows, NZO mice were both β-cell and whole-body insulin resistant while they did not develop liver insulin resistance (Fig. 5.4 A-C). That might be due to the point mutation in the gene encoding for the phosphatidylcholine transfer protein leading to abnormal lipid homeostasis and a decrease of phosphatidylcholine transfer activity in NZO mice[91]. This is interesting and demonstrates that the development of β-cell insulin resistance is not dependent on the presence or parallel development of liver insulin resistance. β-cell insulin resistance in NZO mice as, in ob/ob mice, was paralleled by increased body weight and impaired glucose tolerance (Fig. 5.4. D, E). In contrast to ob/ob mice, an improvement towards older age could not be seen in NZO mice within the actual observation time period.

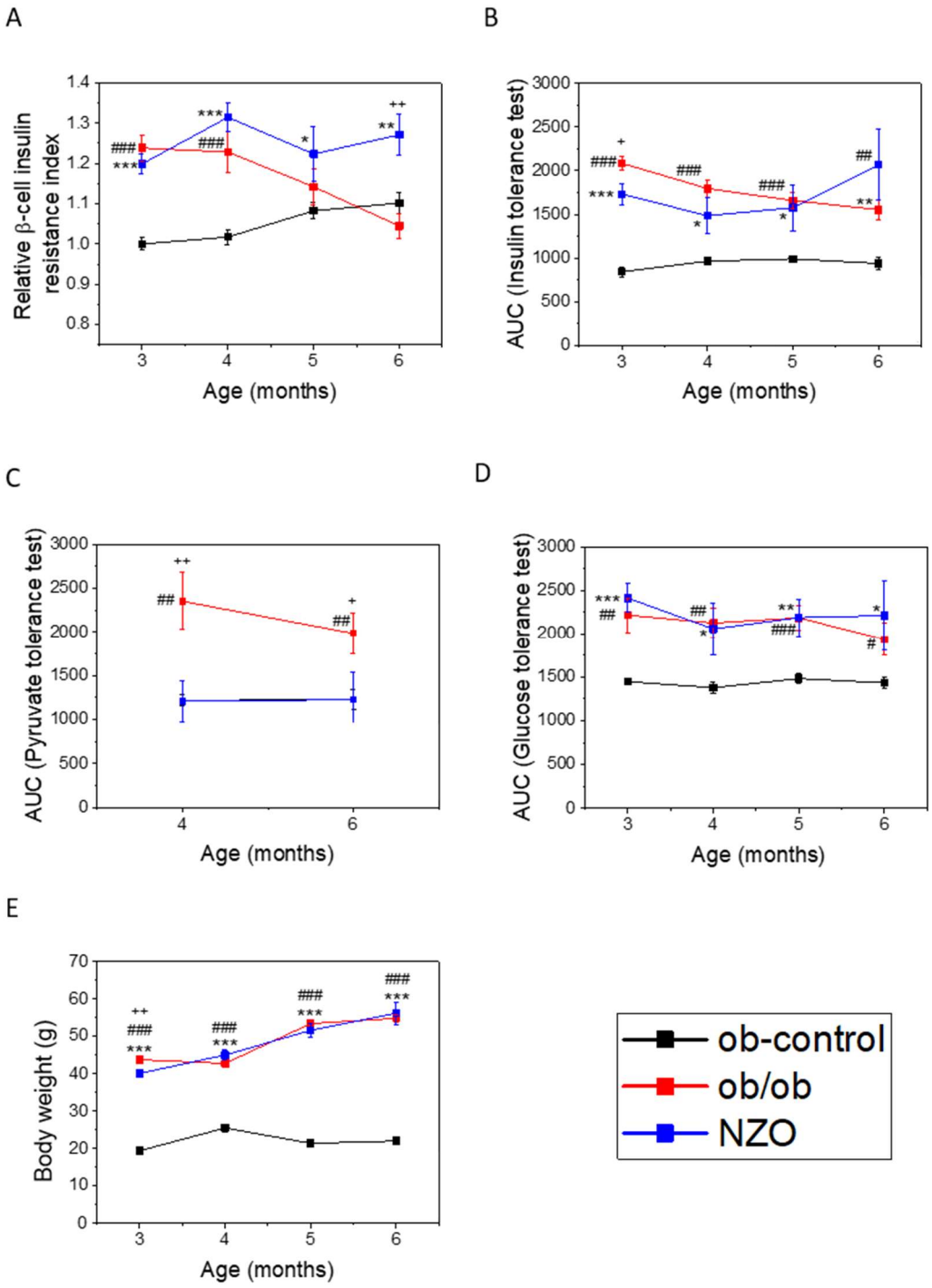

Figure 5.4: Dynamics of insulin resistance and other physiological parameters obtained in NZO mice

(A) β-cell insulin resistance depicted as relative β-cell insulin resistance index obtained with βIRB (n=3-9). (B) Whole-body insulin resistance obtained by the IPITT and depicted as AUC of the individual traces obtained during the IPITT (n=5-10). (C) Liver insulin resistance obtained by the IPPTT and depicted as AUC of the individual traces of the IPPTT (n=5). (D) Glucose tolerance obtained by the IPGTT and depicted as AUC of the individual traces obtained during the IPGTT (n=4). (E) Body weight (n=5).

(A-E) All studies have been conducted with NZO, ob/ob and ob-control mice from 3 to 6 months of age. N-numbers indicated for NZO mice, for n-number of ob/ob and ob-control mice see Fig. 5.3. *p<0.05; **p < 0.01; ***p < 0.001: NZO vs. ob-control. #p<0.05; ##p<0.01; ###p<0.001: ob/ob vs. ob-control. +p<0.05; ++p<0.01: NZO vs. ob/ob. Data are expressed as mean ± SEM.

The genetic mouse models we used to monitor the dynamics of β-cell insulin resistance have the advantage that they had been extensively characterized. We could demonstrate that different dynamics for β-cell insulin resistance exist and that β-cell insulin resistance developed together with whole-body insulin resistance, impaired glucose tolerance and increased body weight, but not necessarily with liver insulin resistance as shown in NZO mice. The disadvantage of genetic animal models is the fact that we could not monitor the onset of insulin resistance by exclusively using *in vivo* imaging of reporter islets in the eye because of the early establishment of the phenotype. Finally, genetic models poorly represent the situation in humans where life style, especially eating behavior, is discussed as one of the most important contributing factors in the development of insulin resistance and T2DM.

5.3 β-cell insulin resistance in diet-induced mouse models

To investigate the relevance of β-cell insulin resistance under conditions that are more relevant to the human situation where eating behavior is thought to affect the development of insulin resistance and T2DM[1,2], we fed metabolic disease prone B6 mice[39] different diets, monitored β-cell insulin resistance with βIRB and obtained other physiological parameters. Since we kept the genetic background constant, we could correlate the outcomes directly to component(s) of the diet. We distinguished between single diets (HSD; HFrD; HFD) and combination diets (HFHSD; HFHFrD). A combination diet (i.e. solid food in combination with sweetened beverages) probably reflects best the eating behavior in humans in respect to fast food consumption. But in general, the transferability of the obtained results and interpretation from mouse to human has to be critically considered. Monitoring β-cell insulin resistance and other physiological parameters in mice fed one of the different diets for 8 weeks revealed that the dynamics of β-cell insulin resistance and other physiological parameters are different (paper II; Tab. 5.1).

Table 5.1: Summary of the physiological parameters obtained in male B6 mice fed different diets

The numbers indicate the week from which on a respective parameter is significantly changed under a certain condition. Unchanged parameters are indicated with a minus.

	HSD	HFrD (Fig.5.5)	HFD	HFHSD	HFHFrD
β-cell insulin resistance	-	not measured	-	**4**	-
Whole-body insulin resistance	-	-	4	**4**	1
Liver insulin resistance	-	-	4	**-**	2
Impaired glucose tolerance	-	-	1	**1**	1
Increased body weight	-	-	2	**4**	1

β-cell insulin resistance did not develop in animals fed a liquid high sugar diet. Both sucrose (paper II, fig. 3) and fructose (Fig. 5.5) feeding in combination with a normal chow diet did not provoke any changes in the obtained parameters. Obviously these mice could adapt their caloric intake as shown in [110], avoiding weight gain and subsequent impairment of glucose and insulin tolerance within the diet intervention period. This is in contrast to the observation that fructose provokes overfeeding in humans (reviewed in [111]). In B6 mice it has been shown before that chow fed mice that were administered fructose- or glucose-supplemented water were similar in physiological measurements[112].

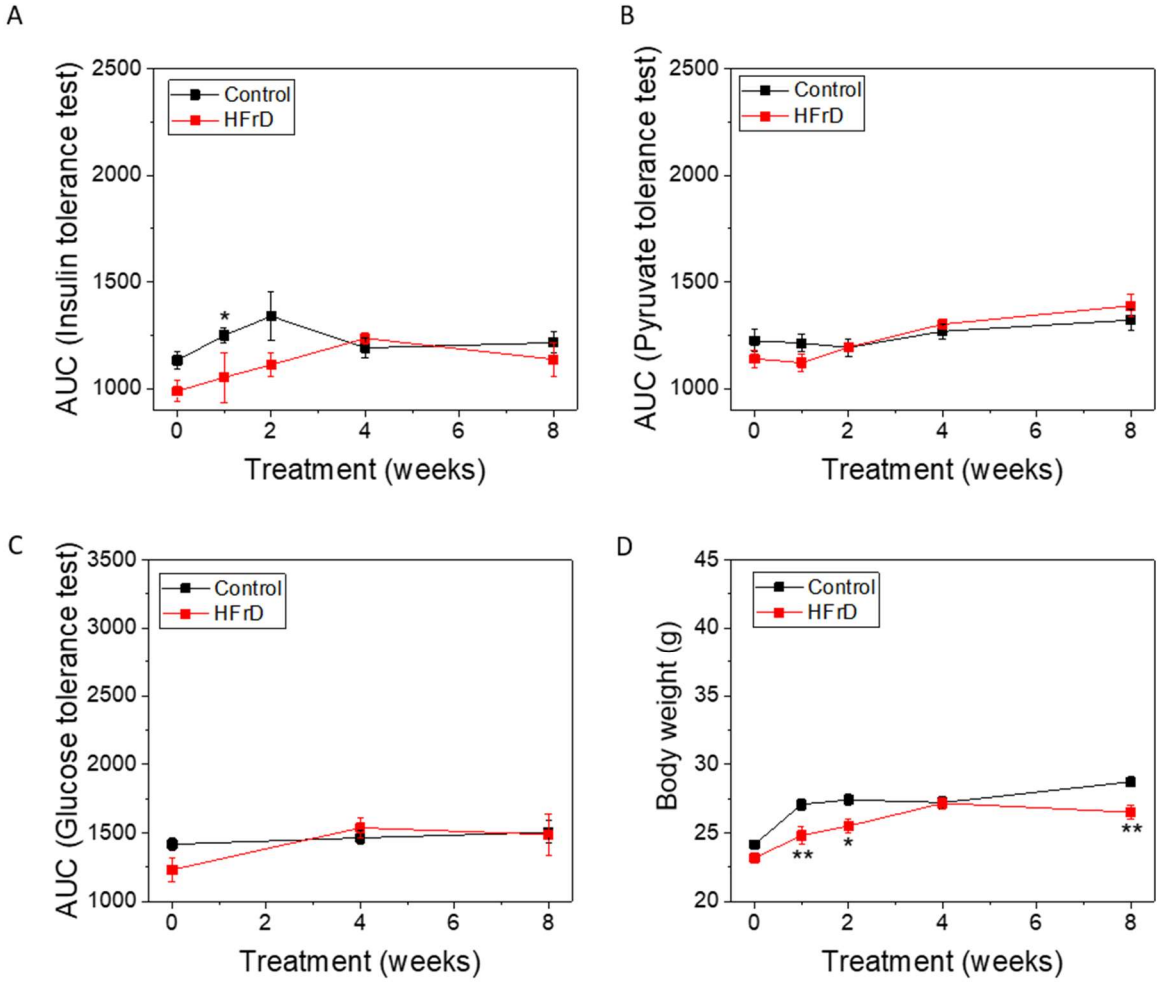

Figure 5.5: Physiological parameters obtained in mice fed a High-Fructose Diet (HFrD)

(A) Whole-body insulin resistance in HFrD and control diet fed B6 mice at 0 to 8 weeks of treatment obtained by intraperitoneal IPITT and depicted as AUC of the IPITT (n=3-6). (B) Liver insulin resistance in HFrD and control diet fed B6 mice at 0 to 8 weeks of treatment obtained by intraperitoneal IPPTT and depicted as AUC of the IPPTT (n=4-5). (C) Glucose tolerance in HFrD and control diet fed B6 mice at 0, 4 and 8 weeks of treatment obtained by intraperitoneal IPGTT and depicted as AUC of the IPGTT (n=6-12). (D) Body weight of HFrD and control diet fed B6 mice at 0 to 8 weeks of treatment (n=5-10). Data shown as mean ± SEM, *p<0.05, **p<0.01.

On the other hand, the administration of a solid diet high in fat led to body weight gain, impaired glucose tolerance, whole-body and liver insulin resistance, but not to β-cell insulin resistance (paper II, fig. 3). Consequently, lipotoxicity alone was not able to induce β-cell insulin resistance within 8 weeks of diet intervention. A HFHFrD also resulted in increased body weight, impaired glucose tolerance, whole-body and liver insulin resistance (paper II, fig. 1). The effects were more pronounced and developed earlier than during a HFD, but β-cell insulin resistance did not develop in these animals.

As shown in paper II, fig. 1 and 2, the combination of a solid diet high in fat and drinking water containing sucrose (HFHSD) led to the development of β-cell insulin resistance within 8 weeks of diet intervention. Sucrose is a disaccharide consisting of fructose and glucose. In contrast to fructose, glucose stimulates the production and secretion of insulin by the β-cell. β-cell insulin resistance was paralleled by whole-body insulin resistance, impaired glucose tolerance and increased body weight. In contrast to mice fed one of the other HFDs (HFD and HFHFrD) these mice did not become liver insulin resistant. Mice receiving a HFHSD might be protected from developing liver insulin resistance due to the glucose provided by the sucrose as it has been reported by others before[112]. There, fructose was shown to be associated with increased hepatic fatty acid synthesis and insulin resistance, while glucose supplementation led to improved insulin signaling in the liver[112]. Our results show that lipotoxicity and high work-load of the β-cell, provoked by glucose stimulation, are necessary for the development of β-cell insulin resistance.

5.3.1 Female and male mice respond differently to a HFHSD

In humans, men are more prone to become diabetic than women[113,114]. Several studies demonstrated that the sex hormone estrogen protects against diabetes[115]. When we fed female B6 mice a HFHSD for 8 weeks we also observed a significant increase in body weight, impaired glucose tolerance and whole-body insulin resistance (Fig. 5.6 B, D, E). The increased body weight and the AUC of the insulin and glucose tolerance tests were comparable to those of male mice fed a control diet. As male B6 mice female mice did not develop liver insulin resistance (Fig 5.6 C), but in contrast to male mice females did not develop β-cell insulin resistance (Fig. 5.6 A). Within in the scope of this thesis work, the mechanisms that protect female mice from developing β-cell insulin resistance were not further investigated. Others have shown that estrogen is able to improve insulin sensitivity and to suppress gluconeogenesis by activation of Estrogen Receptor α-PI3K-Akt-FoxO1 signaling in the liver[116]. If this is also true for the β-cell, it could give one explanation for the observation that female mice did not develop β-cell insulin resistance. Further research will be of importance for the future to obtain deeper insights into the molecular mechanisms underlying the effect of diets and sex differences on β-cell insulin sensitivity.

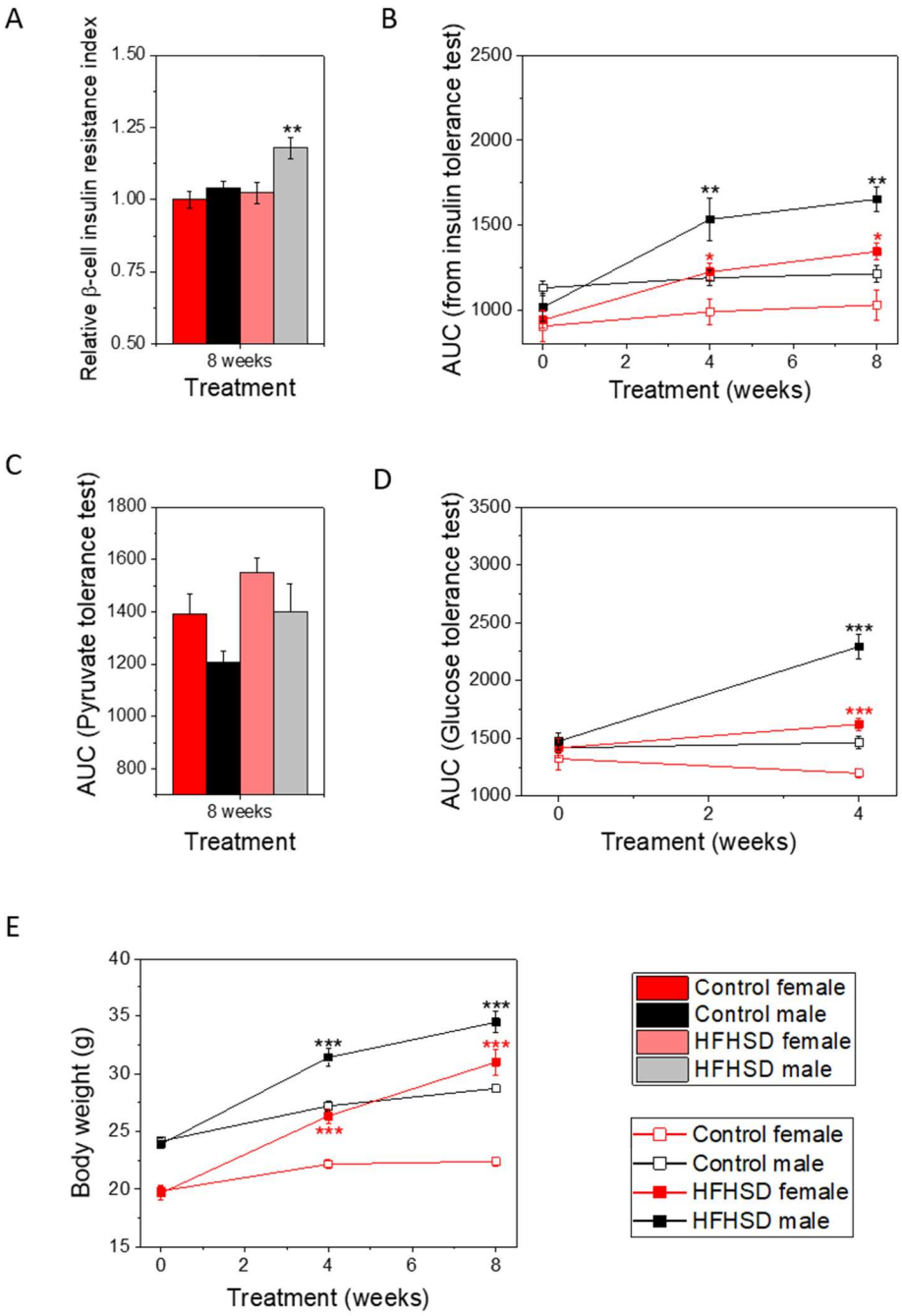

Figure 5.6: Dynamics of insulin resistance and other physiological parameters obtained in female B6 mice fed a HFHSD for 8 weeks

(A) β-cell insulin resistance depicted as relative β-cell insulin resistance index obtained with βIRB at 8 weeks after diet intervention start (n=3-5). (B) Whole-body insulin resistance obtained by the IPITT and depicted as AUC of the individual traces obtained during the IPITT before and during a HFHSD intervention (n=4-6). (C) Liver insulin resistance obtained by the IPPTT and depicted as AUC of the individual traces of the IPPTT at 8 weeks after diet intervention start (n=4-6). (D) Glucose tolerance obtained by the IPGTT and depicted as AUC of the individual traces obtained during the IPGTT before and during a HFHSD intervention (n=4-6). (E) Body weight before and during a HFHSD intervention (n=4-6).

(A-E) n-numbers indicated for female B6 mice receiving a HFHSD, for n-number male B6 see fig. 1 in paper 2. *p<0.05; ***p < 0.001: Female B6 mice receiving a HFHSD versus female B6 mice receiving a control diet. Data are expressed as mean ± SEM.

Taken together we could show that β-cell insulin resistance is also relevant in the context of diet-induced whole-body insulin resistance. The divergent effects of the different diets, also in respect to sex differences, show the complexity of interactions of genetic and environmental factors in the development of T2DM.

5.4 Characteristics of β-cell insulin resistance

Our data have so far demonstrated that β-cell insulin resistance occurs *in vivo* in genetic (ob/ob, NZO) as well as in a diet-induced mouse model of insulin resistance (HFHSD, male B6 mice). Next we aimed to understand the consequences of diet-induced β-cell insulin resistance and started a characterization of underlying molecular mechanisms. Furthermore we investigated a new concept of insulin signaling cascade-selective β-cell insulin resistance.

5.4.1 Diet-induced β-cell insulin resistance is associated with decreased functional β-cell mass

Since the HFHSD led to β-cell insulin resistance in male B6 mice, we further used this animal diet model for investigating the characteristics of β-cell insulin resistance.

5.4.1.1 Functional β-cell mass is decreased during diet-induced β-cell insulin resistance

In order to investigate functional β-cell mass during the development of β-cell insulin resistance, we took again advantage of the *in vivo* imaging platform and a second biosensor, the β-cell fluorescent metabolic transcriptional response indicator (βFLUOMETRI) (fig. 4a in paper II). βFLUOMETRI is a read-out for integrated β-cell function based on the ability of the β-cell to upregulate transcription upon glucose stimulation[67]. It has been demonstrated previously (reviewed in [6]) that the whole cascade of events starting with glucose uptake, metabolism, insulin secretion and insulin binding to the IR as well as proper insulin signaling is necessary for upregulation of the expression of insulin and glucokinase genes in β-cells (paper II, fig. S3a). Both the RIP1 as well as the β-cell-active glucokinase promoter (bGK) were shown to contain metabolic response elements allowing upregulation of promoter activity upon insulin and glucose stimulation *in vitro* ([36,117,118,119]; paper II, fig. 4b). Since we demonstrated that CMV-promoter driven Cerulean was unaffected by insulin and glucose stimulation ([36]; paper II, fig. 4d), we used Cerulean expression for normalization (paper II, fig. 4e). So far the concept of glucose-induced promoter activation had only been shown and used *in vitro*. Our *in vivo* validation of βFLUOMETRI (paper II, fig. 4f; for detailed experimental description see paper II, fig. S3b) demonstrated that we could use this approach to monitor glucose-dependent promoter activation *in vivo*. Because the number of analyzable cells was relatively high, this biosensor allowed us to determine the mass of functional β-cells. To investigate the functional β-cell mass during development and presence of β-cell insulin resistance, we transplanted B6 mice with βFLUOMETRI-expressing reporter islets. One month after transplantation we determined β-cell function as well as other physiological parameters and started a HFHSD. Results in paper II, fig. 5a-h showed that increased body weight, impaired glucose and insulin tolerance as well as β-cell insulin resistance were paralleled by impairment in glucose-stimulated upregulation of promoter activity and a decreasing glucose responding β-cells. The relevance of β-cell insulin sensitivity for maintenance of β-cell mass has been shown before[10], but so far only the absolute β-cell mass irrespectively of functionality could be determined[120]. Here we developed, validated and used a method that allowed measurement of functional β-cell mass longitudinally *in vivo*. Our data revealed that β-cell insulin resistance was associated with a decline in functional β-cell mass.

5.4.1.2 Diet-induced β-cell insulin resistance leads to non-compensatory glucose-stimulated insulin secretion

To study the consequences of diet-induced β-cell insulin resistance, we next examined the metabolic status of mice fed a HFHSD for 8 weeks. HFHSD-fed mice had higher fasting blood glucose as well as higher serum insulin and C-peptide levels compared to mice fed a control diet (paper II, fig. 6a,b,e). Also during a glucose tolerance test these mice secreted higher amounts of insulin and C-peptide (paper II, fig. 6c,f). In contrast to control mice they lacked the ability to further increase secretion upon glucose challenge within the first 5 minutes of the test (paper II, 6d,g and S4). This was in agreement with the results from β-cell function measurements using βFLUOMETRI where both RIP1 and bGK promoter elements did not respond to the glucose challenge. The backscatter signal of engrafted islets, indicative of the insulin content[56], was comparable in reporter islets in HFHSD and control diet fed mice (paper II, fig. 7c), indicating that β-cells of HFHSD mice did not completely deplete their insulin stores in contrast to ob/ob mice. Hence, β-cell insulin resistance provoked a relative defect in insulin secretion that did not compensate hyperglycemia. Insulin secretion deficiency was also observed in genetic KO mouse models of β-cell insulin resistance[10,12,38]. The differences between diet-induced and KO-induced β-cell insulin resistance resulting in relative versus absolute insulin secretion deficiency, respectively, might be due to the complete loss of the target protein in the KO model. The diet intervention can affect a huge range of proteins in the whole body, but may affect those to a lesser extent, thus resulting in less drastic outcome. Nevertheless, the relative defect in insulin secretion provoked by β-cell insulin resistance was sufficient to contribute to a diabetes-like phenotype.

5.4.1.3 The defect in glucose-stimulated insulin secretion is downstream of glucose-stimulated Ca^{2+} influx

To study where in the stimulus-secretion coupling the problem occurs that caused the inability of the β-cell to respond adequately to a glucose challenge, we measured glucose-stimulated β-cell Ca^{2+} excursions in reporter islets in the ACE *in vivo*. For that purpose, we transplanted islets from Ins-Cre:GCaMP3 mice, that express the Ca^{2+} biosensor GCaMP3 in β-cells (Jacob et al., unpublished data), to the ACE of male B6 mice. After engraftment we fed these mice a HFHSD for 8 weeks. The results showed that Ca^{2+} excursions and the amount of cells that were responding upon a glucose challenge were unchanged in these mice (paper II, fig. 7a,b). Consequently the defect in insulin secretion must be downstream of glucose-stimulated Ca^{2+} handling in the β-cells. A failure in insulin exocytosis independent from impaired Ca^{2+} influx was also observed in genetic KO mouse models of β-cell insulin resistance[12,38].

5.4.1.4 Syntaxin-1A is, at least in part, responsible for the defect in glucose-stimulated insulin secretion during diet-induced β-cell insulin resistance

To examine the underlying molecular defects causing non-compensatory glucose-stimulated insulin secretion we performed a biased transcriptomics analysis (qRTPCR) in islets from HFHSD and control diet fed mice at 8 weeks of diet intervention (paper II, fig. 7d). The results showed no gross changes in β-cell identity, because expression of the master regulator of β-cell gene expression Pdx1 and the β-cell-specific activator of the insulin gene MafA was unchanged. Also expression of genes involved in β-cell glucose handling

(GLUT2, glucokinase) was not changed in islets of mice fed a HFHSD for 8 weeks, suggesting that glucose metabolism is not defect. Both gene expression analysis and Western blot analysis identified the SNARE protein syntaxin-1A to be downregulated during β-cell insulin resistance induced by a HFHSD (paper II, fig. 7d,e). The SNARE protein syntaxin-1A is a key-protein in insulin exocytosis[121,122], which binds both insulin granules and L-type voltage gated Ca^{2+} channels[123] to allow glucose-stimulated Ca^{2+} influx close to the release site of insulin. It has been shown before that impaired insulin signaling in β-cells results in a decrease in syntaxin-1A expression[12,124] and that lipotoxicity reduces the association between insulin granules and L-type voltage gated Ca^{2+} channels leading to decreased insulin secretion under conditions of normal glucose-stimulated Ca^{2+} excursions[125,126]. The decrease in syntaxin-1A provided one explanation for the defective glucose-stimulated insulin secretion. Nevertheless, further analysis has to be done to fully characterize insulin resistant β-cells.

5.4.1.5 Diet-induced β-cell insulin resistance is reversible

In ob/ob mice we observed that β-cell insulin resistance could reverse (5.2.). In order to investigate whether dietary-provoked β-cell insulin resistance is also reversible, we fed the mice a normal chow diet after 8 weeks of HFHSD diet intervention. As shown in fig. 5, paper II mice that once received a HFHSD needed 8 weeks to restore their body weight to normal levels. Recovery of glucose tolerance as well as whole-body and β-cell insulin tolerance took only 4 weeks. These results clearly showed that β-cell insulin resistance is reversible. The recovered β-cell insulin sensitivity was paralleled by improved insulin and glucose tolerance. Furthermore, it was accompanied by regain of functional β-cell mass. Since β-cells were transduced with βFLUOMETRI prior to transplantation, we can be sure that the same β-cells re-gained their function. Recovery from β-cell insulin resistance was independent from increased body weight, but occurred when also the body weight decreased. A remaining question for the future will be to investigate whether a “point-of-no-return” exists, i.e. a status of β-cell insulin resistance from which the β-cell is unable to recover.

5.4.2 Insulin signaling cascade-selective β-cell insulin resistance can lead to a re-routing of insulin signaling

A broad variety of insulin signaling pathways exists that form the two major branches, i.e. mitogenic and metabolic insulin signaling. In these signaling cascades adaptor proteins act as the interphase between the activated IR and the downstream effector proteins. They channel the insulin signal to different signaling pathways leading to different biological effects[127]. In the β-cell, the following adaptor proteins have been identified: IR substrate (IRS) proteins IRS-1 to IRS-6, Shc, APS, $p62^{dok}$ and Gab-1 and members of the PI3K family[6]. As we define insulin resistance as any possible disturbance in insulin signaling, β-cell insulin resistance can exist in one specific signaling pathway, while other insulin signaling cascades remain intact. The knockdown of the IR-B adaptor protein PI3K-C2α led to a higher interaction of IR-B with Shc, resulting in decreased metabolic signaling and increased mitogenic signaling, thus re-routing the insulin signal from metabolic to mitogenic signaling (paper III; Fig. 5.7).

5.4.2.1 PI3K-C2α knockdown leads to increased mitogenic insulin signaling and β-cell proliferation

To analyze the consequences of insulin signaling cascade specific β-cell insulin resistance, we performed siRNA-mediated knockdown of PI3K-C2α. The IR-B adaptor protein PI3K-C2α regulates among others the expression of the β-cell glucose sensor glucokinase. The lipid product of PI3K-C2α ($PI(3,4)P_2$) leads to activation of Akt which phosphorylates downstream members of the insulin signaling cascade such as TBC1D4 and FoxO1. The results showed that knockdown of PI3K-C2α led to increased proliferation in MIN6 cells, mouse and human primary β-cells (paper III, fig. 1d-f, S1) as well as decreased apoptosis in MIN6 cells (paper III, fig. 1g,h, S2). Furthermore we analyzed the phosphorylation status of FoxO1 and TSC2 and could show that both proteins were less phosphorylated and thereby in an activated state (paper III, fig. S3a,b). These results showed that metabolic insulin signaling was decreased. Since proliferation might be associated with mitogenic insulin signaling we next analyzed two members of the mitogenic insulin signaling cascade, ERK 1/2 and c-*fos*. The results revealed an increase in ERK 1/2 phosphorylation, c-*fos* promoter activity and c-*fos* protein expression (paper III, fig. 2a-c). Taken together a knockdown of PI3K-C2α led to a decrease in metabolic and an increase in mitogenic insulin signaling, accompanied by an increase in β-cell proliferation.

5.4.2.2 PI3K-C2α knockdown leads to a re-routing from metabolic to mitogenic pathway via higher interaction of IR-B and Shc

In order to investigate the mechanism by which the β-cell is able to change from a differentiated to a proliferative state by switching from metabolic to mitogenic insulin signaling, we first aimed to understand which IR is involved. We employed a pan-antibody that blocked both IR isoforms and an antibody that specifically blocks IR-B. Furthermore, we used aptamers that allowed specific inhibition of IR-A and -B. Since only blocking of IR-B or both IRs, but not blocking of IR-A only, abolished the increase in proliferation after PI3K-C2α knockdown of mouse and human β-cells (paper III, fig. 2d-g), we concluded that the switch did not occur from IR-B to IR-A signaling, but a re-routing of the signal from a metabolic to a mitogenic pathway downstream of IR-B. Furthermore we employed reporter gene constructs as read-out for both pathways, i.e. expression of GFP under the control of

bGK promoter (metabolic pathway via IR-B/ PI3K-C2α) and DsRed under the c-*fos* promoter (mitogenic pathway via IR-B/Shc/ERK)[37,99]. PI3K-C2α knockdown resulted in increased c-*fos* promoter-driven DsRed expression while bGK promoter-driven GFP expression was decreased (paper III, fig. 2i). It remained to analyze how the β-cell mechanistically was able to upregulate signaling via the mitogenic pathway upon PI3K-C2α knockdown. To address this question we studied the interaction between IR-B and Shc by co-immunoprecipitation and FRET. Both techniques showed a higher association between IR-B and Shc when PI3K-C2α was knocked down (paper III, fig. 3a-c). The results demonstrated that PI3K-C2α knockdown led to higher interaction of IR-B and Shc which re-routed the insulin signal from the metabolic IR-B/PI3K-C2α pathway to signaling via a mitogenic pathway involving IR-B/Shc/ERK (Fig. 5.7.).

5.4.2.3 Re-routing occurs in the diabetic and *in vivo* context

Next we wanted to investigate if the above described mechanism can also occur under diabetic conditions and *in vivo*. MIN6 cells were incubated with increasing glucose concentrations (2 mM, 11 mM, 25 mM; for 24 hours), mimicking hyperglycemic conditions found in diabetes. Figure 3d and e (paper III) show that prolonged elevated glucose levels provoked a higher association between IR-B and Shc as well as increased proliferation. Since previous studies had shown that ob/ob mice at 3 months of age display an insulin resistant phenotype we analyzed protein expression and interaction in islet lysates of 3 months old ob/ob and control mice with Western blot and immunoprecipitation, respectively. The results showed that glucokinase expression was decreased while protein levels of c-*fos*, ERK and Shc were increased (paper III, fig. 4a-g). Furthermore the interaction of IR-B with Shc was increased in islets of ob/ob mice compared to control mice (paper III, fig. 4h-j). Immunostaining showed that proliferating β-cells, indicated by positive KI-67 staining, had lower levels of PI3K-C2α (paper III, fig. S4). Also in mice fed a HFHSD for 8 weeks we could observe β-cell proliferation indicated by an increased BrdU incorporation in β-cells and an increase in islet size in the ACE (paper II, fig. S6). Furthermore we observed a trend towards decreased PI3K-C2α and increased Shc gene expression (paper II, fig. 7d). Future work has to explore whether PI3K-C2α protein levels are decreased and Shc levels are increased in these animals as well. These results clearly demonstrated that re-routing of insulin signaling as the result of selective β-cell insulin resistance could be relevant in the diabetic context and in the situation of β-cell insulin resistance *in vivo*.

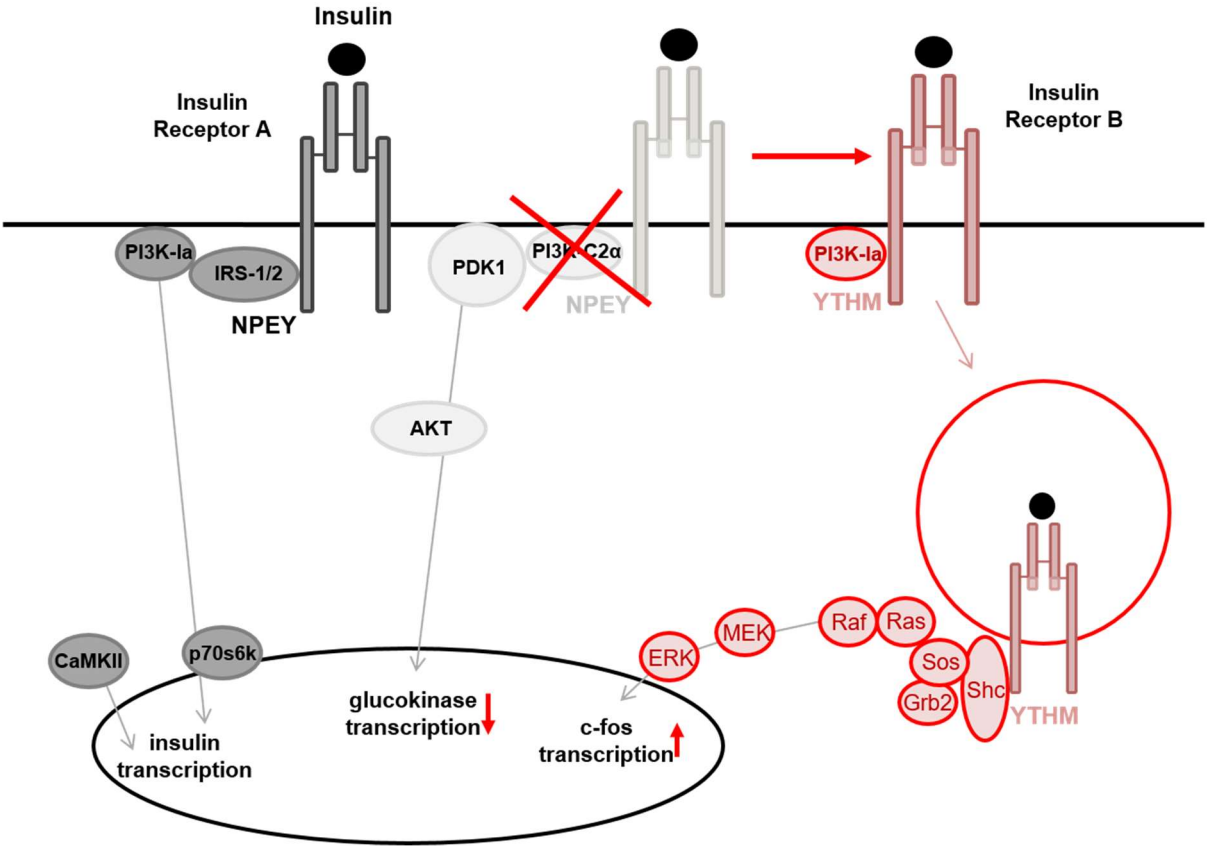

Figure 5.7.: Re-routing of insulin signaling

PI3K-C2α knockdown leads to higher interaction of IR-B with Shc resulting in a decrease in metabolic insulin signaling and an increase in mitogenic signaling associated with increased β-cell proliferation.

6 CONCLUSIONS

1. **β-cell insulin resistance** can be measured non-invasively and longitudinally *in vivo* employing the *in vivo* imaging platform and the βIRB.
2. **β-cell insulin resistance** dynamics vary in different mouse models of insulin resistance.
   β-cell insulin resistance develops in the presence of whole-body insulin resistance, impaired glucose tolerance and increased body weight, but does not require the development of liver insulin resistance.
3. **β-cell insulin resistance** is relevant in the context of diet-induced insulin resistance and develops in male B6 mice fed a HFHSD.
4. **β-cell insulin resistance** in HFHSD-fed male B6 mice is accompanied by decreased functional β-cell mass and impaired insulin secretion due to a failure downstream of glucose-stimulated Ca^{2+} influx, in part due to a reduction of syntaxin-1A.
   β-cell insulin resistance in one insulin signaling cascade can lead to re-routing of the insulin signal, thus explaining the co-existence of reduced and increased insulin responses in the same cell.

7 FUTURE PERSPECTIVE

The results of this thesis work show the relevance of β-cell insulin resistance in the context of diet-induced insulin resistance. Male B6 mice fed a HFHSD for eight weeks developed β-cell insulin resistance due to lipotoxicity induced by the solid diet high in fat (60%) and the high β-cell work-load provoked by the drinking water containing a high percentage of sucrose (32%). Analysis of the underlying molecular consequences of β-cell insulin resistance revealed a defect in glucose-stimulated insulin secretion, which we could track to a failure downstream of the glucose-stimulated Ca^{2+} influx in β-cells. This was, at least in part, due to the downregulation of syntaxin-1A gene expression and reduced protein levels (paper II). These outcomes were in agreement with previous observations obtained in genetically-induced models of β-cell insulin resistance[12,38]. Employing βIRB had the advantage that β-cells could specifically be analyzed non-invasively in the living animal and followed longitudinally *in vivo* (paper I and II). In contrast to that, for gene expression and protein analysis whole islets were used, containing all pancreatic islet cell types. Since 50 to 80% of cells in mouse islets of Langerhans are β-cells[20], we are confident that the obtained results are relevant and contribute to the understanding of β-cell insulin resistance, but future work should aim for single-cell gene expression and protein analysis of insulin resistant β-cells. This would require labeling of insulin resistant β-cells with β-cell specific makers, e.g. Pdx1 or βIRB, followed by sorting, e.g. by fluorescence activated cell sorting (FACS), before analysis. In paper III we demonstrated that β-cells that are insulin resistant in one signaling pathway can re-route the insulin signal from a metabolic to mitogenic insulin signaling pathway. So far, we do not know, if the same β-cells that are insulin resistant, as indicated by βIRB, also show re-routing, i.e. a downregulation in PI3K-C2α and proliferation. This question could be addressed with the analysis of sorted insulin resistant β-cells. In line with the literature on sub-populations of β-cells[128–130], also sub-populations of insulin resistant β-cells may be identified. This would not be unexpected since several insulin signaling pathways act in parallel in the β-cell[6] and consequently a defect in insulin signaling can occur at different steps within these insulin signaling cascades, leading to different β-cell defects.

Both the genetic predisposition as well as environmental factors have been shown to contribute to the risk to develop diabetes[26]. As we used the same mouse model (male C57BL/6J) in the current diet intervention study, we could relate the distinct dynamics of insulin resistance and diabetes progression to the particular diets. HFD, HFHSD and HFHFrD caused impaired glucose tolerance and whole-body insulin resistance, but only a HFHSD provoked β-cell insulin resistance (paper II). By showing that differences in diet-induced diabetes development exist, probably depending on different underlying molecular mechanisms, this study supports the notion of sub-categories of T2DM[24]. Understanding the sub-categories of diabetic patients would allow personalized, specific and especially improved treatment regimens for patients.

Our results demonstrate that β-cell dysfunction occurred early after start of the diet-intervention, i.e. within 4-8 weeks of diet intervention (paper II). This observation is not new[131], but stands in contrast to the current view on T2DM development, where it is

believed that β-cell failure occurs late as a result of chronic exhaustion. So far, we have observed that β-cell insulin resistance was always accompanied by impaired glucose tolerance. Blood glucose levels may therefore still be the gold standard for the diagnosis of (pre)diabetes, but identification of markers for β-cell insulin resistance is likely to contribute to defining sub-categories of diabetic patients and thereby to more specific therapies.

The results obtained in our studies underscore the relevance and huge impact of diet composition as an environmental factor for (pre)diabetes development and the importance of prevention programs in terms of life style awareness contributing to a decrease in new diabetes cases. Irrespectively of the genetic background, a healthy life style can delay or even prevent diabetes progression[27,28]. WHO and IDF have set the goal to promote a healthy life style, including physical activity and a healthy diet[1,2]. Taken together, personalized prevention strategies adapted to the variability in diabetes development and sub-forms should be a way to contain the diabetes pandemic. Moreover, people should receive more support in everyday life to keep a healthy life style[132,133].

In conclusion, improved methods to study β-cell insulin resistance and its consequences and a better understanding of β-cell insulin resistance itself can improve prevention and treatment strategies in the struggle against T2DM.

8 ACKNOWLEDGEMENTS

During the last years I have been on an extraordinary journey through the field of science. I am grateful for the experiences made. A lot of people have contributed and helped me to finalize this thesis. In particular I like thank the following people:

My supervisors **Ingo** and **Barbara Leibiger** for setting up and supervising these research projects, sharing your research and life experiences. I always enjoyed discussions about research, life, the current world situation and so much more. Ingo, I am impressed by your inexhaustible flow of new ideas for new research projects and I thank you for your optimism. Barbara, thank you for bringing down all these ideas to realistic projects and always being critical! Thank you for introducing me into the field of ornithology! In future I will probably never see a bird without wondering what its name is!

My co-supervisor **Per-Olof Berggren** for an excellently equipped lab, an extraordinary work environment and your enthusiasm about *in vivo* work, your critical comments on my work and for reading my thesis!

My dear coworker and colleague **Tilo Moede**, I thank you so much for basically everything! You have guided me all these years through all the ups and downs, you have shared your knowledge about microscopy, the academic world and how to survive along this journey!

My mentor **Jochen Schwenk** and **Andrea Nuß** for your time to listen to my worries, always giving me the feeling that you are there to support me!

Ismael Valladolid-Acebes for all your help with experiments and measurements. Thank you for honest discussions about my results and science!

Noah Moruzzi for being enthusiastic in contributing to the projects.

Kerstin Brismar your interest in my research projects and my person.

My co-authors, not mentioned so far: **Galyna Bryzgalova**, **Stefan Jacob**, **Jong Hoon Lim**, **Teresa Pereira**, **Sung Ho Rye**, **Na-Oh Yunn**, **Concha F. García-Prieto** for your contribution to the respective publications.

For help with administrative things in the lab, research projects or Ph.D. education: **Katarina Breitholtz**, **Yvonne Strömberg**, **Monica Isaksson**, **Ann-Britt Wikström**, **Kerstin Florell**, **Britt-Marie Witasp, Therese Kindåker, Amalia Kewenter**.

Jan-Erik Kaare, Zebastian Ahlberg and **Thomas Westerberg** for your help with the computers when they did not want to work as intended.

My former and present PhD-student colleagues **Subu Surendran Rajasekaran**, **Teresa Daraio**, **Pim van Krieken**, **Karin Åvall**, **Sampath Narayanan**, **Yue Shi**, **Saad Al-Qahtani**, **Yixin Wang**, **Robin Fröbom**, **Muhammad Irfan**, **Cheng Xu** and **Sofie Eliasson**. Thank you for nice discussions during the PhD-meetings and culinary journeys during dinners!

All present and former colleagues in the Rolf Luft Centrum not mentioned so far: **Chris Barker**, **Elisabetta Dare**, **Andrea Dicker**, **Erwin Ilegems, Lisa Juntti-Berggren, Martin Köhler, Elisabeth Noren-Krog, Jaehong Park, Essam Refai, Michèle Sorgenfrei, Philip Tröster, Montserrat Visa Majoral, Anya Voznesenskaya, Yan Xiong, Shao-Nian Yang, Jia Yu, Lina Yu, Irina Zaitseva, Sergei Zaitsev, Kaixuan Zhao, Neil Portwood**, **Thusita Paluwatte Muhandiramlage**, **Massimiliano Ria**, **Nancy Dekki Shalaly**, **Lars Selander**, **Yusuf Ali**, **Tomas Alanentalo, Ulrika Johansson**, **Sergiu-Bogdan Catrina, Gustav Dallner, Christina Bark**, **Jacob Grünler, Xiao-Wei Zheng, Anette Landström, Ishrath Ansurudeen**, **Magnus Bentinger**, **Michael Tekle**. Furthermore the guest students from Brazil: **Thais, Fernando, Karen**, **Anderson**, **Eduardo**, **Sabrina**.

People from the labs in Miami and Singapore for their critical comments during weekly lab meetings.

The whole **staff at AKM** for your help with the mice.

All the mice that gave their life for research, new insights into the β-cells and not at least for my thesis.

A lot of people have supported me during my childhood, in school, at university, during my internships in Wuppertal and Hamburg and my time in Stockholm. You gave me the feeling that I should be as I am. My thanks go to:

Familie Bertok, **Familie Paschen**, **Familie Vermöhlen**, **Familie Mühlbach**, **Oma Rosi und Opa Willi**

Maren and **Martin Münier** for your trust when you let me take care of **Merle** and **Maura** by that I early experienced responsibility. I thank you for all your visits, the uncountable amount of postcards I received during all these years and your interest in my person and my further development! **Maren**, thank you for the music ;-)!

Janine Preuße, my first biology (and music) teacher in school, who has become an important tutor in my life, for your support through all these years, for your visits in Stockholm and endless honest discussion about life!

My host families in Canterbury (England), Moscow (Russia) and Campinas (Brazil) for experiencing different countries and cultures while staying with you!

Astrid Lindgren for the books that made me dream about Sweden!

My old classmate **Inga Kirsch** for all your e-mails, your visit in Stockholm and all the nice words you had for me when questioning myself and life.

My "**Lübeck-Mädels**", **Fiona**, **Karen**, **Kathi**, **Linda**, **Maymi**, **Sonja** and **Sophie**, without them I would had never enjoyed my studies at Lübeck University with so much fun and friendship. It is nice still being in contact with all of you and to meet you once in a while.

All people I met in the **KSG Lübeck**, especially **Karl Schultz** for becoming a role model when it became my turn to arrange group evenings for young people. **Prälat Patrick**

Boland for sharing your knowledge during evening meetings and presentations, but also for an unforgettable week in Rome 2009.

Maetzel family, thank you all for your trust in my person and being a family for me during university time. Thank you for your open home and hearts for me and my beloved ones!

Alla som pratat svenska med mig under de senaste åren. Att jag har utvecklat mina språkkunskaper betyder mycket för mig. Såklart kommer processen aldrig att ta slut, så var vänlig och korrigera fel använda prepositioner och allt annat även i framtiden!

Steffi Bölter, for the first months in Stockholm and your continuous friendship! Du är toppen!

All people I met in the German Church's Community. Already from my first week in Sweden on I felt home in the heart of Gamla Stan. Thanks to all the generations of "Top20s" during the last years bringing me down to the little problems of everyday life. To all people that I met in different groups and for different occasions (do not feel sad that I will not mention you all, the risk forgetting someone is too high, thanks for your understanding!). **Lisa Guggomos** for your friendship and the nice times being together! My special thanks goes to my dear friend **Sandra Schwebe** being a really good partner during the last years, for all the evenings we spent on planning, ending up in talking about so many others things.

All the friendly musicians from "**Flauto Notte**", "**Flauto Sera**" and "**Flauto Alba**"/"**Flauto Dia**" I met in "Heidis musikskola". Regular repetitions, many nice concerts and concert tours (a particular breakfast on Åland will never be forgotten ;-)!) gave me the opportunity to think about something completely different once in a while and gave both me and Tilo the feeling of being welcome at any time. Especially I like to thank **Heidi Rohlin Westin**, for your endless energy to come up with new projects and ideas. Thank you and Flauto Sera that you followed my suggestion to have an exchange with my old ensemble from Flensburg!

Uta Hardt and **Florian Schober** for nice cooking and game-playing evenings!

Pernilla and Tord Ringenhall for your friendship and the nice time we spent together!

All the wonderful "Sopplunch" people from Centrumskyrkan. You have shown me what really counts in life and that creativity as well as community are so important to feed hungry people.

Camilla Olofsson for your friendship during the last years, for all the (lunch) hours spending together talking about PhD-studies, live and so much more.

Karen Grütz for your friendship, a lot of skype calls and your deep understanding of my worries about so much!

My dear friend and witness **Edith Sturm** for our time in Stockholm and all the skype calls thereafter, you are always missed when walking in Haga Parken and around Säbysjön!

Sonja Müller-Krumkamp for your deep friendship, the monthly/weekly telephone calls as well as the days we spent together.

My family-in-law, the **Moedes** and **Moede-Noltings**, for our nice times together.

Dank meinen Großeltern **Katharina** und **Josef Bertok** für all die liebevoll gepackten Päckchen gefüllt mit Tee, selbstgebackenen Plätzchen, gefüllten Waffeln oder Kuchen, nicht zuletzt auch Eure Besuche in Stockholm. Ihr wisst gar nicht, wie viel das alles bedeutet hat!

My parents **Klaus** and **Beate Paschen** for your endless love and the freedom you gave me to follow my dreams, supporting me whatever decision I made.

My sister **Silke Paschen** for your understanding for your older sister, all your visits in Stockholm bringing sun in my life in so many ways ;-)

My beloved husband **Tilo Moede** for your love, optimism and trust. You did not want to have a long section, so I make it short, putting all my gratitude in these three words: Oi, oi, oi!

My son **Vitus Moede Paschen** for just being there and behaving brilliant during your first months of life, supporting me with enough sleep, uncountable smiles and the feeling that life after completing the thesis will continue with new exiting things every single day!

This thesis was supported by funds from the Karolinska Institutet (KID programme), the Swedish Research Council, the Family Erling-Persson Foundation, the Novo Nordisk Foundation, Novo Nordisk A/S, the Stichting af Jochnick Foundation, the Swedish Diabetes Association, Scandia Insurance Company Limited, the Diabetes Research and Wellness Foundation, the Berth von Kantzow's Foundation, the Strategic Research Program in Diabetes at Karolinska Institutet, the ERC-2013-AdG 338936 BetaImage, the ERC2017-PoC 727306 BETASCREEN, the Swedish Foundation for Strategic Research, and the Knut and Alice Wallenberg Foundation. N.M. was supported by a Novo Nordisk postdoctoral fellowship run in partnership with the Karolinska Institutet.

9 REFERENCES

1. World Health Organization. *Global Report on Diabetes*. (2016).
2. IDF Diabetes Atlas, 7th edition. ISBN: 978-2-930229-81-2 (2015).
3. Malik, V. S. *et al.* Sugar-Sweetened Beverages and Risk of Metabolic Syndrome and Type 2 Diabetes. *Diabetes Care* **33,** 2477–2483 (2010).
4. Feero, W. G., Guttmacher, A. E. & Mccarthy, M. I. Genomic Medicine Genomics, Type 2 Diabetes, and Obesity. *N. Engl. J. Med.* **363,** 2339–50 (2010).
5. Bajaj, M. & DeFronzo, R. A. Metabolic and molecular basis of insulin resistance. *J. Nucl. Cardiol.* **10,** 311–323 (2003).
6. Leibiger, I. B., Leibiger, B. & Berggren, P.-O. Insulin Signaling in the Pancreatic β-cell. *Annu. Rev. Nutr* **28,** 233–51 (2008).
7. Kulkarni, R. N. *et al.* Tissue-Specific Knockout of the Insulin Receptor in Pancreatic β-cells Creates an Insulin Secretory Defect Similar to that in Type 2 Diabetes. *Cell* **96,** 329–339 (1999).
8. Bernal-Mizrachi, E., Wen, W., Stahlhut, S., Welling, C. M. & Permutt, M. A. Islet β-cell expression of constitutively active Akt1 / PKB α induces striking hypertrophy, hyperplasia, and hyperinsulinemia. *J. Clin. Invest.* **108,** 1575–1576 (2001).
9. Hashimoto, N. *et al.* Ablation of PDK1 in pancreatic β-cells induces diabetes as a result of loss of β-cell mass. *Nat. Genet.* **38,** 589–593 (2006).
10. Cantley, J. *et al.* Pancreatic deletion of insulin receptor substrate 2 reduces β- and α-cell mass and impairs glucose homeostasis in mice. *Diabetologia* **50,** 1248–1256 (2007).
11. Okada, T. *et al.* Insulin receptors in β-cells are critical for islet compensatory growth response to insulin resistance. *Proc. Natl. Acad. Sci. U. S. A.* **104,** 8977–8982 (2007).
12. Kaneko, K. *et al.* Class IA Phosphatidylinositol 3-Kinase in Pancreatic β-cells Controls Insulin Secretion by Multiple Mechanisms. *Cell Metab.* **12,** 619–632 (2010).
13. Speier, S. *et al.* Noninvasive in vivo imaging of pancreatic islet cell biology. *Nat Med.* **14,** 574–8 (2008).
14. Speier, S. *et al.* Noninvasive high-resolution in vivo imaging of cell biology in the anterior chamber of the mouse eye. *Nat Protoc.* **3,** 1278–1286 (2008).
15. Ilegems, E. *et al.* Reporter islets in the eye reveal the plasticity of the endocrine pancreas. *Proc. Natl. Acad. Sci. U. S. A.* **110,** 20581–6 (2013).
16. Palmer, A. E., Qin, Y., Park, J. G. & McCombs, J. E. Design and application of genetically encoded biosensors. *Trends Biotechnol.* **29,** 144–152 (2011).
17. Ni, Q., Mehta, S. & Zhang, J. Live-cell imaging of cell signaling using genetically encoded fluorescent reporters. *FEBS J.* **285,** 203–219 (2017).
18. Bolbat, A. & Schultz, C. Recent developments of genetically encoded optical

sensors for cell biology. *Biol. Cell* **109,** 1–23 (2017).

19. Rennie, J. & Fraser, T. THE ISLETS OF LANGERHANS IN RELATION TO DIABETES. *Bio-Chemical J.* 7–19 (1906).

20. Islam, S. *Islet of Langerhans*. (Springer Science+Business Media Dordrecht, 2015).

21. Stenström, G., Gottsäter, A., Bakhtadze, E., Berger, B. & Sundkvist, G. Latent autoimmune diabetes in adults: Definition, prevalence, β-cell function, and treatment. *Diabetes* **54,** S68–S72 (2005).

22. Czech, M. P. Insulin action and resistance in obesity and type 2 diabetes. *Nat Med* **23,** 804–814 (2017).

23. Sah, S. P., Singh, B., Choudhary, S. & Kumar, A. Animal models of insulin resistance: A review. *Pharmacol. Reports* **68,** 1165–1177 (2016).

24. Ahlqvist, E. *et al.* Novel subgroups of adult-onset diabetes and their association with outcomes: a data-driven cluster analysis of six variables. *Lancet Diabetes Endocrinol.* **8587,** 1–9 (2018).

25. Dirar, A. M. & Doupis, J. Gestational diabetes from A to Z. *World J. Diabetes* **8,** 489–506 (2017).

26. Franks, P. W. & Merino, J. Gene-lifestyle interplay in type 2 diabetes. *Curr. Opin. Genet. Dev.* **50,** 35–40 (2018).

27. Brown, S. A., García, A. A., Zuñiga, J. A. & Lewis, K. A. Effectiveness of workplace diabetes prevention programs: A systematic review of the evidence. *Patient Educ. Couns.* **101,** 1036–1050 (2018).

28. American Diabetes Association. Prevention or delay of type 2 diabetes: Standards of medical care in Diabetes-2018. *Diabetes Care* **41,** S51–S54 (2018).

29. Ahima, R. S. & Lazar, M. A. The Health Risk of Obesity—Better Metrics Imperative. *Science.* **341,** 856–858 (2013).

30. Brereton, M. F., Vergari, E., Zhang, Q. & Clark, A. Alpha-, Delta- and PP-cells. *J. Histochem. Cytochem.* **63,** 575–591 (2015).

31. Ashcroft, F. M. *et al.* Stimulus-Secretion Coupling in Pancreatic β-cells. *J. Cell. Biochem.* **55,** 54–65 (1994).

32. Seino, S., Seinot, M., Nishi, S. & Bell, G. I. Structure of the human insulin receptor gene and characterization of its promoter. *Proc. Natl. Acad. Sci. U. S. A.* **86,** 114–118 (1989).

33. Ullrich, A. *et al.* Human insulin receptor and its relationship to the tyrosine kinase family of oncogenes. *Nature* **313,** 756–761 (1985).

34. Ebina, Y. *et al.* The human insulin receptor cDNA: The structural basis for hormone-activated transmembrane signalling. *Cell* **40,** 747–758 (1985).

35. Leibiger, B. *et al.* Short-term regulation of insulin gene transcription by glucose. *Proc. Natl. Acad. Sci. U. S. A.* **95,** 9307–9312 (1998).

36. Leibiger, I. B., Leibiger, B., Moede, T. & Berggren, P.-O. Exocytosis of Insulin Promotes Insulin Gene Transcription via the Insulin Receptor/PI-3 Kinase/p70 s6 Kinase and CaM Kinase Pathways. *Mol. Cell* **1,** 933–938 (1998).

37. Uhles, S., Moede, T., Leibiger, B., Berggren, P.-O. & Leibiger, I. B. Selective gene activation by spatial segregation of insulin receptor B signaling. *FASEB J.* **21,** 1609–1621 (2007).

38. Bernal-Mizrachi, E. *et al.* Defective insulin secretion and increased susceptibility to experimental diabetes are induced by reduced Akt activity in pancreatic islet β-cells. *J. Clin. Invest.* **114,** 928–936 (2004).

39. Kulkarni, R. N. *et al.* Impact of Genetic Background on Development of Hyperinsulinemia and Diabetes in Insulin Heterozygous Mice. *Biosystems* **52,** (2003).

40. Kaku, K., Fiedorek, F. T., Province, M. & Permutt, M. A. Genetic Analysis of Glucose Tolerance in Inbred Mouse Strains: Evidence for Polygenic Control. *Diabetes* **37,** 707–713 (1988).

41. Carter, M. E. & Brunet, A. Quick guide FOXO transcription factors. *Curr. Biol.* **17,** 113–114 (2007).

42. Zhang, T. *et al.* FoxO1 Plays An Important Role in Regulating β-cell Compensation for Insulin Resistance in Male Mice. *Endocrinology* **157,** 1055–70 (2016).

43. Martinez, S. C., Cras-Méneur, C., Bernal-Mizrachi, E. & Permutt, M. A. Glucose regulates FoxO1 through insulin receptor signaling in the pancreatic islet beta-cell. *Diabetes* **55,** 1581–1591 (2006).

44. Kawamori, D. *et al.* The forkhead transcription factor FoxO1 bridges the JNK pathway and the transcription factor PDX-1 through its intracellular translocation. *J. Biol. Chem.* **281,** 1091–1098 (2006).

45. Gan, L., Zheng, W., Chabot, J. G., Unterman, T. G. & Quirion, R. Nuclear/cytoplasmic shuttling of the transcription factor FoxO1 is regulated by neurotrophic factors. *J. Neurochem.* **93,** 1209–1219 (2005).

46. Kitamura, Y. I. *et al.* FoxO1 protects against pancreatic β-cell failure through NeuroD and MafA induction. *Cell Metab.* **2,** 153–163 (2005).

47. Olbrot, M., Rud, J., Moss, L. G. & Sharma, A. Identification of β-cell-specific insulin gene transcription factor RIPE3b1 as mammalian MafA. *Proc. Natl. Acad. Sci. U. S. A.* **99,** 6737–6742 (2002).

48. Ahlgren, U., Jonsson, J. & Jonsson, L. β-cell-specific inactivation of the mouse Ipf1 / Pdx1 gene results in loss of the β -cell phenotype and maturity onset diabetes. *Genes Dev.* **12,** 1763–1768 (1998).

49. Kitamura, T. *et al.* The forkhead transcription factor FoxO1 links insulin signaling to Pdx1 regulation of pancreatic β-cell growth. *J. Clin. Invest.* (2002).

50. Dooremaal, dr. J. C. van. Die Entwicklung der in fremden Grund versetzten lebenden Gewebe. *Albr. von Graefes Arch. fur Klin. und Exp. Ophthalmol.* **19,** 358–373 (1873).

51. Adeghate, E. & Donáth, T. Morphological findings in long-term pancreatic tissue transplants in the anterior eye chamber of rats. *Pancreas* **5,** 298–305 (1990).

52. Abdulreda, M. H., Rodriguez-Diaz, R., Caicedo, A. & Berggren, P. O. Liraglutide compromises pancreatic β-cell function in a humanized mouse model. *Cell Metab.* **23,** 541–546 (2016).

53. Adeghate, E. Pancreatic tissue grafts are reinnervated by neuro-peptidergic and

cholinergic nerves within five days of transplantation. *Transpl. Immunol.* **10,** 73–80 (2002).

54. Rodriguez-Diaz, R., Speier, S., Damaris, R., Formoso, A. & Gans, I. Noninvasive in vivo model demonstrating the effects of autonomic innervation on pancreatic islet function. *Proc. Natl. Acad. Sci. U. S. A.* **109,** 21456–21461 (2012).

55. Rodriguez-Diaz, R. *et al.* Paracrine Interactions within the Pancreatic Islet Determine the Glycemic Set Point. *Cell Metab.* **27,** 549–558.e4 (2018).

56. Ilegems, E. *et al.* Light scattering as an intrinsic indicator for pancreatic islet cell mass and secretion. *Sci. Rep.* **5,** 10740 (2015).

57. Abdulreda, M. H. *et al.* High-resolution, noninvasive longitudinal live imaging of immune responses. *Proc. Natl. Acad. Sci. U. S. A.* **108,** 12863–12868 (2011).

58. Li, G. *et al.* Multifunctional *in vivo* imaging of pancreatic islets during diabetes development. *J. Cell Sci.* **129,** 2865–2875 (2016).

59. Schneider, A. F. L. & Hackenberger, C. P. R. Fluorescent labelling in living cells. *Curr. Opin. Biotechnol.* **48,** 61–68 (2017).

60. Shimomura, O., Johnson, F. H. & Saiga, Y. Extraction, Purification and Properties of Aequorin, a Bioluminescent Protein from the Luminous Hydromedusan, Aequorea. *J. Cell. Comp. Physiol* **59,** 223–239 (1962).

61. Prasher, D. C., Eckenrode, V. K., Ward, W. W., Prendergast, F. G. & Cormier, M. J. Primary structure of the Aequorea victoria green-fluorescent protein. *Gene* **111,** 229–233 (1992).

62. Chalfie, M., Tu, Y., Euskirchen, G., Ward, W. W. & Prasher, D. C. Green Fluorescent Protein as a Marker for Gene Expression. *Science.* **263,** 802–805 (1994).

63. Miyawaki, A. *et al.* Fluorescent indicators for Ca 2+ based on green fluorescent proteins and calmodulin. *Nature* **388,** 882–887 (1997).

64. Tsien, R. Y. The green fluorescent protein. *Annu. Rev. Biochem* **67,** 509–44 (1998).

65. Sanford, L. & Palmer, A. Recent Advances in Development of Genetically Encoded Fluorescent Sensors. *Methods Enzymol.* **589,** 1–49 (2017).

66. Frommer, W. B., Davidson, M. W. & Campbell, R. E. Genetically encoded biosensors based on engineered fluorescent proteins. *Chem. Soc. Rev.* **38,** 2833 (2009).

67. Moede, T., Leibiger, B., Berggren, P.-O. & Leibiger, I. B. Online Monitoring of Stimulus-Induced Gene Expression in Pancreatic β-cells. *Diabetes* **50,** S15–S19 (2001).

68. Förster, T. Zwischenmolekulare Energiewanderung und Fluoreszenz. in *Annalen der Physik* **2,** 55–75 (1948).

69. Miyazaki, J.-I. *et al.* Establishment of a Pancreatic β-cell Line That Retains Glucose-Inducible Insulin Secretion: Special Reference to Expression of Glucose Transporter Isoforms. *Endocrinology* **127,** 126–132 (1990).

70. Graham, F. L., Smileyt, J., Russell, W. C. & Nairn, R. Characteristics of a Human Cell Line Transformed by DNA from Human Adenovirus Type 5. *J Gen Virol.* **36,** 59–7 (1977).

71. Moore, G. E., Gerner, R. E. & Franklin, H. A. Culture of normal human leukocytes. *J. Am. Med. Assoc.* **199,** 519–524 (1967).

72. Goto, M. *et al.* Refinement of the automated method for human islet isolation and presentation of a closed system for in vitro islet culture. *Transplantation* **78,** 1367–75 (2004).

73. Zhao, X. *et al.* Multiple elements regulate nuclear/cytoplasmic shuttling of FOXO1: characterization of phosphorylation-and 14-3-3-dependent and -independent mechanisms. *Biochem. J* **378,** 839–849 (2004).

74. Shaner, N. C. *et al.* Improved monomeric red, orange and yellow fluorescent proteins derived from Discosoma sp. red fluorescent protein. *Nat. Biotechnol.* **22,** 1567–1572 (2004).

75. Uhles, S., Moede, T., Leibiger, B., Berggren, P.-O. & Leibiger, I. B. Isoform-specific insulin receptor signaling involves different plasma membrane domains. *J. Cell Biol.* **163,** 1327–1337 (2003).

76. Sefah, K., Shangguan, D., Xiong, X., O, M. B. & Tan, W. Development of DNA aptamers using Cell-SELEX. *Nat. Protoc.* **5,** 1169–1185 (2010).

77. Cousin, S. P. *et al.* Free Fatty Acid-Induced Inhibition of Glucose and Insulin-Like Growth Factor I-Induced Deoxyribonucleic Acid Synthesis in the Pancreatic beta-Cell Line INS-1. *Endocrinology* **142,** 229–240 (2001).

78. Ingalls, A. M., Dickie, M. M. & Snell, G. D. Obese, a new mutation in the house mouse. *Obes. Res.* **4,** 101 (1996).

79. Batt, R. & Mialhe, P. Insulin resistance in the inherently obese mouse-obob. *Nature* **212,** 289–290 (1966).

80. Zhang, Y. *et al.* Positional cloning of the mouse obese gene and its human homologue. *Nature* **372,** 425–432 (1994).

81. Friedman, J. M. & Halaas, J. L. Leptin and the regulation of body weight in mammals. *Nature* **395,** 763–770 (1998).

82. Funcke, J.-B. *et al.* Monogenic forms of childhood obesity due to mutations in the leptin gene. *Mol. Cell. Pediatr.* **1,** 1–8 (2014).

83. Ellett, J. D., Evans, Z. P., Zhang, G., Chavin, K. D. & Spyropoulos, D. D. A rapid PCR-based method for the identification of ob mutant mice. *Obesity* **17,** 402–404 (2009).

84. Lindström, P. The Physiology of Obese-Hyperglycemic Mice [ob/ob Mice]. *Sci. World J.* **7,** 666–685 (2007).

85. Åvall, K. *et al.* Apolipoprotein CIII links islet insulin resistance to β-cell failure in diabetes. *Proc. Natl. Acad. Sci. U. S. A.* 201423849 (2015).

86. Coleman, D. L. & Hummel, K. The Influence of Genetic Background on the Expression of the Obese. *Diabetologia* **9,** 287–293 (1973).

87. Bielschowsky, M. & Goodall, C. M. Origin of Inbred NZ Mouse Strains. *Cancer Res.* **30,** 834–836 (1970).

88. Leiter, E. H. *et al.* NIDDM Genes in Mice Deleterious Synergism by Both Parental Genomes Contributes to Diabetogenic Thresholds. *Diabetes* **47,** 1287–1295 (1998).

89. Larkins, R. G. Defective Insulin Secretory Response to Glucose in the New Zealand Obese Mouse Improvement with Restricted Diet. *Diabetes* **22,** 251–255 (1973).

90. Igel, M., Becker, W., Herberg, L. & Joost, H. Hyperleptinemia, Leptin Resistance, and Polymorphic Leptin Receptor in the New Zealand Obese Mouse. *J. Mol. Endocrinol.* **21,** 337–45 (1998).

91. Pan, H. J. *et al.* A polymorphism in New Zealand inbred mouse strains that inactivates phosphatidylcholine transfer protein. *FEBS Lett.* **580,** 5953–5958 (2006).

92. Kluth, O. *et al.* Dissociation of lipotoxicity and glucotoxicity in a mouse model of obesity associated diabetes: Role of forkhead box O1 (FOXO1) in glucose-induced β-cell failure. *Diabetologia* **54,** 605–616 (2011).

93. Defronzo, R. A., Tobin, J. D. & Andreas, R. Glucose clamp technique: a method for quantifying insulin secretion and resistance. *Am. J. Physiol.* **237,** E214-223 (1979).

94. Karpova, T. & McNally, J. G. Detecting Protein-Protein Interactions with CFP-YFP FRET by Acceptor Photobleaching. in *Current Protocols in Cytometry* 12.7.1.-12.7.11 (2006).

95. Thorens, B. *et al.* Ins1 Cre knock-in mice for β-cell-specific gene recombination. *Diabetologia* **58,** 558–565 (2015).

96. Zariwala, H. A. *et al.* Cellular/Molecular A Cre-Dependent GCaMP3 Reporter Mouse for Neuronal Imaging In Vivo. *J. Neurosci.* **32,** 3131–3141 (2012).

97. Edelstein, A., Amodaj, N., Hoover, K., Vale, R. & Stuurman, N. Computer Control of Microscopes Using μManager. in *Curr. Protoc. Mol. Biol* 14.20.1-14.20.17 (2010).

98. Leibiger, B. *et al.* Selective Insulin Signaling through A and B Insulin Receptors Regulates Transcription of Insulin and Glucokinase Genes in Pancreatic β-Cells. *Mol. Cell* **7,** 559–570 (2001).

99. Leibiger, B. *et al.* Insulin-feedback via PI3K-C2alpha activated PKBalpha/Akt1 is required for glucose-stimulated insulin secretion. *FASEB J.* **24,** 1824–1837 (2010).

100. Van Krieken, P. P. *et al.* Kinetics of functional β-cell mass decay in a diphtheria toxin receptor mouse model of diabetes. *Sci. Rep.* **7,** 12440 (2017).

101. Boutet de Monvel, J., Le Calvez, S. & Ulfendahl, M. Image Restoration for Confocal Microscopy: Improving the Limits of Deconvolution, with Application to the Visualization of the Mammalian Hearing Organ. *Biophys. J.* **80,** 2455–2470 (2001).

102. Guizar-Sicairos, M., Thurman, S. T. & Fienup, J. R. Efficient subpixel image registration algorithms. *Opt. Lett.* **33,** 156 (2008).

103. Zanella, R. *et al.* Towards real-time image deconvolution: application to confocal and STED microscopy. *Sci. Rep.* **3,** 2523 (2013).

104. Kroon, D.-J. Segmentation of the Mandibular Canal in Cone-Beam CT Data. (University of Twente, 2011).

105. Schmittgen, T. D. & Livak, K. J. Analyzing real-time PCR data by the comparative C T method. *Nat. Protoc.* **3,** 1101–1108 (2008).

106. Buteau, J. & Accili, D. Regulation of pancreatic beta-cell function by the forkhead

protein FoxO1. *Diabetes, Obes. Metab.* **9,** 140–146 (2007).

107. Gan, L., Zheng, W., Chabot, J.-G., Unterman, T. G. & Quirion, R. Nuclear/cytoplasmic shuttling of the transcription factor FoxO1 is regulated by neurotrophic factors. *J. Neurochem.* **93,** 1209–1219 (2005).

108. Tang, E. D., Nuñez, G., Barr, F. G. & Guan, K.-L. Negative Regulation of the Forkhead Transcription Factor FKHR by Akt. *J. Biol. Chem.* **274,** 16741–16746 (1999).

109. Chen, C. *et al.* Alterations in β-cell calcium dynamics and efficacy outweigh islet mass adaptation in compensation of insulin resistance and prediabetes onset. *Diabetes* **49,** db151718 (2016).

110. Lindqvist, A., De La Cour, C. D., Stegmark, A., Håkanson, R. & Erlanson-Albertsson, C. Overeating of palatable food is associated with blunted leptin and ghrelin responses. *Regul. Pept.* **130,** 123–132 (2005).

111. Elliott, S. S., Keim, N. L., Stern, J. S., Teff, K. & Havel, P. J. Fructose, weight gain, and the insulin resistance syndrome. *Am. J. Clin. Nutr.* **76,** 911–22 (2002).

112. Softic, S. *et al.* Divergent effects of glucose and fructose on hepatic lipogenesis and insulin signaling. *J. Clin. Invest.* **127,** 4059–4074 (2017).

113. Sattar, N. Gender aspects in type 2 diabetes mellitus and cardiometabolic risk. *Best Pract. Res. Clin. Endocrinol. Metab.* **27,** 501–507 (2013).

114. Wändell, P. E. & Carlsson, A. C. Gender differences and time trends in incidence and prevalence of type 2 diabetes in Sweden—A model explaining the diabetes epidemic worldwide today? *Diabetes Res. Clin. Pract.* **106,** e90–e92 (2014).

115. Liu, S. & Mauvais-Jarvis, F. Minireview: Estrogenic Protection of β-cell Failure in Metabolic Diseases. *Endocrinology* **151,** 859–864 (2010).

116. Yan, H. *et al.* Estrogen Improves Insulin Sensitivity and Suppresses Gluconeogenesis via the Transcription Factor Foxo1. *Diabetes* (2018). doi:10.2337/db18-0638

117. Melloul, D., Marshak, S. & Cerasi, E. β-cell-specific expression of the insulin gene. *Diabetologia* **45,** 309–326 (2002).

118. Lawrence, M. C., Bhatt, H. S., Watterson, J. M. & Easom, R. A. Regulation of Insulin Gene Transcription by a Ca 2+-Responsive Pathway Involving Calcineurin and Nuclear Factor of Activated T Cells. *Mol. Endocrinol.* **15,** 1758–1767 (2001).

119. Hay, C. W. & Docherty, K. Comparative Analysis of Insulin Gene Promoters Implications for Diabetes Research. *Diabetes* **55,** 3201–3213 (2006).

120. Laurent, D. *et al.* Pancreatic β-cell imaging in humans: Fiction or option? *Diabetes, Obes. Metab.* **18,** 6–15 (2016).

121. Rorsman, P. & Ashcroft, F. M. Pancreatic beta-cell electrical activity and insulin secretion: Of mice and men. *Physiol Rev* **98,** 117–214 (2018).

122. Lam, P. P. L. *et al.* Transgenic Mouse Overexpressing Syntaxin-1A as a Diabetes Model. *Diabetes* **54,** 2744–2754 (2005).

123. Yang, S.-N. *et al.* Syntaxin 1 interacts with the L D subtype of voltage-gated Ca 2+ channels in pancreatic β-cells. *Proc. Natl. Acad. Sci. U. S. A.* **96,** 10164–10169 (1999).

124. Gerdes, J. M. *et al.* Ciliary dysfunction impairs beta-cell insulin secretion and promotes development of type 2 diabetes in rodents. *Nat. Commun.* **5,** (2014).

125. Hoppa, M. B. *et al.* Chronic Palmitate Exposure Inhibits Insulin Secretion by Dissociation of Ca 2+ Channels from Secretory Granules. *Cell Metab.* **10,** 455–465 (2009).

126. Collins, S. C. *et al.* Progression of Diet-Induced Diabetes in C57BL6J Mice Involves Functional Dissociation of Ca 2+ Channels From Secretory Vesicles. *Diabetes* **59,** 1192–1201 (2010).

127. Virkamäki, A., Ueki, K. & Kahn, C. R. Protein-protein interaction in insulin signaling and the molecular mechanisms of insulin resistance. *J. Clin. Invest.* (1999). doi:10.1172/JCI6609

128. Johnston, N. R. *et al.* β-cell Hubs Dictate Pancreatic Islet Responses to Glucose. *Cell Metab.* **24,** 1–13 (2016).

129. Bonner-Weir, S. & Aguayo-Mazzucato, C. Pancreatic beta-cell heterogeneity revisited. *Nature* **535,** 365–366 (2016).

130. Meulen, T. Van Der *et al.* Virgin β-cells Persist throughout Life at a Neogenic Niche within Pancreatic Islets. *Cell Metab.* **25,** 911–926 (2017).

131. Stamateris, R. E., Sharma, R. B., Hollern, D. A. & Alonso, L. C. Adaptive β-cell proliferation increases early in high-fat feeding in mice, concurrent with metabolic changes, with induction of islet cyclin D2 expression. *Am. J. Physiol. Endocrinol. Metab.* **305,** E149-59 (2013).

132. Pays, W. H. O. & In, T. Consumers´ Response to an On-Shelf Nutrition Labelling System in Supermarkets: Evidence to Inform Plocy and Practice. *Growth (Lakeland)* **93,** 1–5 (2010).

133. Tierney, M., Gallagher, A. M., Giotis, E. S. & Pentieva, K. An online survey on consumer knowledge and understanding of added sugars. *Nutrients* **9,** 1–13 (2017).

10 ARTICLES I-III